Amine-Chelated Aryllithium Reagents—Structure and Dynamics

Hans J. Reich,* Wayne S. Goldenberg, Birgir Ö. Gudmundsson, Aaron W. Sanders, Klaus J. Kulicke, Katya Simon, and Ilia A. Guzei†

Contribution from the Department of Chemistry, University of Wisconsin, Madison, Wisconsin 53706

Received February 22, 2001

Abstract: Multinuclear NMR studies of five-membered-ring amine chelated aryllithium reagents 2-lithio-*N*,*N*-dimethylbenzylamine (**1**), the diethylamine and diisopropylamino analogues (**2**, **3**), and the *o*-methoxy analogue (**4**), isotopically enriched in ^{6}Li and ^{15}N, have provided a detailed picture of the solution structures in ethereal solvents (usually in mixtures of THF and dimethyl ether, ether, and 2,5-dimethyltetrahydrofuran). The effect of cosolvents such as TMEDA, PMDTA, and HMPA has also been determined. All compounds are strongly chelated, and the chelation is not disrupted by these cosolvents. Reagents **1**, **2**, and **3** are dimeric in solvents containing a large fraction of THF. Below −120 °C, three chelation isomers of the dimers are detectable by NMR spectroscopy: one (**A**) with both nitrogens coordinated to one lithium of the dimer, and two (**B** and **C**) in which each lithium bears one chelating group. Dynamic NMR studies have provided rates and activation energies for the interconversion of the **1**-**A**, **1**-**B**, and **1**-**C** isomers. They interconvert either by simple ring rotation, which interconverts **B** and **C**, or by amine decoordination (probably associative, $\Delta G^{\ddagger}_{-93} = 8.5$ kcal/mol), which can interconvert all of the isomers. The dimers of **1** are thermodynamically more stable than those of model systems such as phenyllithium, *o*-tolyllithium, or 2-isoamylphenyllithium (**5**, $\Delta\Delta G \geq 3.3$ kcal/mol). They are not detectably deaggregated by TMEDA or PMDTA, although HMPA causes partial deaggregation. The dimers are also more robust kinetically with rates of interaggregate exchange, measured by DNMR line shape analysis of the C−Li signal, orders of magnitude smaller than those of models ($\Delta\Delta G^{\ddagger} \geq 4.4$ kcal/mol). Similarly, the mixed dimer of **1** and phenyllithium, **13**, is kinetically more stable than the phenyllithium dimer by >2.2 kcal/mol. X-ray crystal structures of the TMEDA solvate of **1**-**A** and the THF solvate of **3**-**B** showed them to be dimeric and chelated in the solid state as well. Compound **4**, which has a methoxy group ortho to the C−Li group, differs from the others in being only partially dimeric in THF, presumably for steric reasons. This compound is fully deaggregated by 1 equiv of HMPA. Excess HMPA leads to the formation of ca. 15% of a triple ion (**4**-**T**) in which both nitrogens appear to be chelated to the central lithium.

Introduction

The recognition by Hauser in 1963[1] that the dimethylaminomethyl group could facilitate the metalation of otherwise unreactive ortho aryl hydrogens (e.g., to form **1** from *N*,*N*-dimethylbenzylamine) provided the impetus for a large body

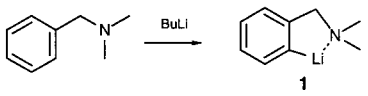

1

of work aimed at exploiting the synthetic utility of chelating effects and understanding the role chelation plays in the formation, structures, and reactions of such lithium reagents. Aryl, vinyl, and even unactivated alkyl hydrogens can be metalated when suitable chelation is provided.[2a,3,4a,5] Chelation effects have been used not only to prepare useful lithium reagents but also to provide structural rigidity to control the stereochemistry of the formation and reactions of lithium reagents[6,7a,8−12] as well as provide structural models for solvation.[4] Despite the importance of these effects, there is relatively

* Address correspondence to this author.

† Inquiries about the X-ray crystallographic studies should be directed to this author.

(1) (a) Jones, F. N.; Zinn, M. F.; Hauser, C. R. *J. Org. Chem.* **1963**, *28*, 663−665. (b) Jones, F. N.; Hauser, C. R. *J. Org. Chem.* **1962**, *27*, 701−702.

(2) (a) Beak, P.; Meyers, A. I. *Acc. Chem. Res.* **1986**, *19*, 356−363. Beak, P.; Snieckus, V. *Acc. Chem. Res.* **1982**, *15*, 306−312. Beak, P.; Zajdel, W. J.; Reitz, D. B. *Chem. Rev.* **1984**, *84*, 471−523. (b) Beak, P.; Kerrick, S. T.; Gallagher, D. J. *J. Am. Chem. Soc.* **1993**, *115*, 10628−10636. (c) Al-Aseer, M.; Beak, P.; Hay, D.; Kempf, D. J.; Mills, S.; Smith S. G. *J. Am. Chem. Soc.* **1983**, *105*, 2080−2082.

(3) Gschwend, H. W.; Roderiguez, H. R. *Org. React.* **1979**, *26*, 1−360.

(4) (a) Klumpp, G. W. *Recl. Trav. Chim. Pays-Bas* **1986**, *105*, 1−21. (b) Schmitz, R. F.; Schakel, M.; Vos, M.; Klumpp, G. W. *Chem. Commun.* **1998**, 1099−1100. (c) Vos, M.; de Kanter, F. J. J.; Schakel, M.; van Eikema Hommes, N. J. R.; Klumpp, G. W. *J. Am. Chem. Soc.* **1987**, *109*, 2187−2188. (d) Klumpp, G. W.; Vos M.; de Kanter, F. J. J.; Slob, C.; Krabbendam, H.; Spek, A. L. *J. Am. Chem. Soc.* **1985**, *107*, 8292−8294. Moene, W.; Vos, M.; de Kanter, F. J. J.; Klumpp, G. W. *J. Am. Chem. Soc.* **1989**, *111*, 3463−3465. Geurink, P. J. A.; Klumpp, G. W. *J. Am. Chem. Soc.* **1986**, *108*, 538−539.

(5) (a) Snieckus, V. *Chem. Rev.* **1990**, *90*, 879−933 and references therein. (b) Slocum, D. W.; Jennings, C. A. *J. Org. Chem.* **1976**, *41*, 3653−3664.

(6) Lamothe, S.; Chan, T. H. *Tetrahedron Lett.* **1991**, *32*, 1847−1850. Hartley, R. C.; Lamothe, S.; Chan, T. H. *Tetrahedron Lett.* **1993**, *34*, 1449−1452.

(7) (a) Myers, A. G.; McKinstry, L. *J. Org. Chem.* **1996**, *61*, 2428−2440. (b) Meyers, A. I.; Riecker, W. F.; Fuentes, L. M. *J. Am. Chem. Soc.* **1983**, *105*, 2082−2083.

(8) Rein, K.; Goicoechea-Pappas, M.; Anklekar, T. V.; Hart, G. C.; Smith, G. A.; Gawley, R. E. *J. Am. Chem. Soc.* **1989**, *111*, 2211−2217.

(9) Klein, S.; Marek, I.; Poisson, J.-F.; Normant, J.-F. *J. Am. Chem. Soc.* **1995**, *117*, 8853−8854.

(10) Riant, O.; Samuel, O.; Flessner, T.; Taudien, S.; Kagan, H. B. *J. Org. Chem.* **1997**, *62*, 6733−6745.

(11) Bowles, P.; Clayden, J.; Tomkinson, M. *Tetrahedron Lett.* **1995**, *36*, 9219−9222.

(12) Hoppe, D.; Gonschorrek, C. *Tetrahedron. Lett.* **1987**, *28*, 785−788.

10.1021/ja010489b CCC: $20.00
Published on Web 07/28/2001

little detailed mechanistic and structural information on the hundreds of organolithium reagents for which chelated structures have been proposed.[2b,c,4d,7b,13a,14,15a−e]

This paper deals with the solution structure and dynamics of chelated lithium reagents **1**−**4**, as well as model system **5**. Previous workers have reported solution NMR studies[14a,16] as well as solid-state X-ray studies[14a,b] of compound **1** and the more soluble *p*-methyl analogue **6**. Analogues with many other metals including B,[17a] Mg,[1a] Al,[17b] Sn,[14c] and Zn[17c] have also been investigated. The X-ray structure of crystals of **1** grown from ether−hexane showed it to be tetrameric,[14a] resembling the structure of PhLi,[18,19] except that the amino group replaces the coordinated ether molecule on each Li atom. Solution studies were performed on the methyl analogue **6**.[14a] In toluene or diethyl ether, the tetrameric structure and N-chelation of **6** remain intact, as evident from the ipso carbon signal at 176.0 ppm with a line width corresponding to about a 12 Hz $^{13}C-(^{7}Li)_3$ coupling and diastereotopic methyl signals of the NMe_2 groups. Upon addition of a small amount of THF (1 equiv per Li) to a toluene or ether solution of tetrameric **6**, a new species was formed with an ipso carbon signal (septet at 189.2 ppm, $^{1}J(^{13}C-^{7}Li) = 20$ Hz) which suggested a dimeric structure.[19a,20] Since the NMe_2 ^{13}C signals were not diastereotopic and had a chemical shift much like those of *N*,*N*-dimethylbenzylamine, van Koten and co-workers suggested that in THF the intramolecular N−Li coordination has been broken.[14a] They drew similar conclusions about the effect of TMEDA. We report here studies of **1** and several analogues at much lower temperatures and using isotopically enriched materials which show that chelation remains intact under all conditions.[15a,b]

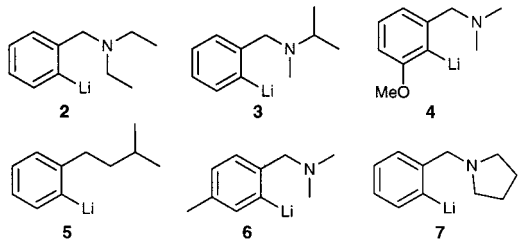

Our investigation was aimed at probing the existence and strength of chelation effects, as well as effects on reactivity patterns. Impetus was provided by several observations. First was the discovery that a propargyllithium reagent **8** with a well-placed 2-pyridyl group was only partially chelated in THF,[15c] analogous to the report that **6** easily lost chelation when a strong donor solvent such as THF or TMEDA was added.[14a] Similarly, the lithium reagent **9** had an allenyl structure in THF solution,[15c] even though the propargyl structure (**10**) could enjoy the benefits of bidentate chelation of a type frequently proposed in the literature.[10,13a,21] These observations cast doubt on the common assumption that lithium reagents with suitably placed pendant basic groups were normally chelated.

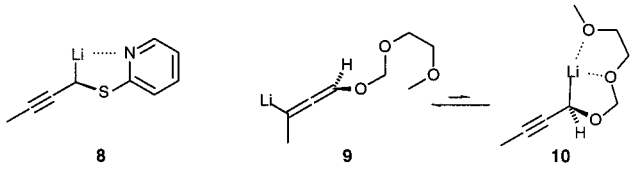

A second impetus for this research was the discovery that virtually all aryllithium reagents formed significant fractions of triple ions, Ar_2Li^- $Li(HMPA)_4^+$, in the presence of HMPA.[15d] We hypothesized that ortho chelating groups might enhance the stability of such structures (e.g., **1**-**T**, **4**-**T**) and allow more effective study of these interesting dimers.

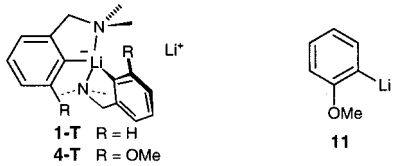

Results and Discussion

In addition to reexamining the previously studied Hauser compound **1**, we also studied the diethylamino (**2**) and isopropylmethylamino (**3**) analogues. We were unable to address the question of chelation in the triple ion of **1** (**1**-**T**) because not enough was formed. Since 2-methoxyphenyllithium and 2,6-dimethoxyphenyllithium give unusually large amounts of triple ions in THF−HMPA solution,[15d] we examined the *o*-methoxy analogue **4** to address the question of chelation in the triple ion **4**-**T**. We will report separately on the pyrrolidine analogue of **1**, compound **7**, as well as the higher homologues with longer side chains and the analogous ether-chelated systems.[15b]

Syntheses. Crystalline samples of **1** were prepared as reported[1a] by metalating *N*,*N*-dimethylbenzylamine with *n*-BuLi in ether at room temperature. Compound **4** was available by metalation of 3-methoxy-*N*,*N*-dimethylbenzylamine,[5b] allowing

(13) (a) Fraenkel, G.; Qiu, F. *J. Am. Chem. Soc.* **1997**, *119*, 3571−3579. (b) For many organolithium reagents, especially aggregated ones, quadrupolar broadening is severe enough with ^{7}Li (92.6% natural abundance) that C−Li coupling cannot be resolved. The ^{6}Li analogues show little or no quadrupolar broadening, and thus couplings are more easily seen. Fraenkel, G.; Fraenkel, A. M.; Geckle, M. J.; Schloss, F. *J. Am. Chem. Soc.* **1979**, *101*, 4745−4747. (c) Jones, A. J.; Grant D. M.; Russell, J. G.; Fraenkel, G. *J. Phys. Chem.* **1969**, *73*, 1624−1626. (d) For an insightful discussion of dynamic processes involving C−Li multiplets in monomeric aryllithium reagents, see: Fraenkel, G.; Subramanian, S.; Chow, A. *J. Am. Chem. Soc.* **1995**, *117*, 6300−6307.

(14) (a) Jastrzebski, J. T. B. H.; van Koten, G.; Konijn, M.; Stam, C. H. *J. Am. Chem. Soc.* **1982**, *104*, 5490−5492. Wehman, E.; Jastrzebski, J. T. B. H.; Ernsting, J.-M.; Grove, D. M.; van Koten, G. *J. Organomet. Chem.* **1988**, *353*, 145−155. (b) Rietveld, M. H. P.; Wehman-Ooyevaar, I. C. M.; Kapteijn, G. M.; Grove, D. M.; Smeets, W. J. J.; Kooijman, H.; Spek, A. L.; van Koten, G. *Organometallics* **1994**, *13*, 3782−3787. (c) van Koten, G.; Noltes, J. G. *J. Am. Chem. Soc.* **1976**, *98*, 5393−5395. (d) Jastrzebski, J. T. B. H.; van Koten, G.; Goubitz, K.; Arlen, C.; Pfeffer, M. *J. Organomet. Chem.* **1983**, *246*, C75−C79.

(15) (a) For the preliminary communication, see: Reich, H. J.; Gudmundsson, B. Ö. *J. Am. Chem. Soc.* **1996**, *118*, 6074−6075. (b) Reich, H. J.; Goldenberg, W. S.; Sanders, A. W.; Tzschucke, C. C. *Org. Lett.* **2001**, *3*, 33−36. (c) Reich, H. J.; Holladay, J. E. *J. Am. Chem. Soc.* **1995**, *117*, 8470−8471. (d) Reich, H. J.; Sikorski, W. H.; Gudmundsson, B. Ö.; Dykstra, R. R. *J. Am. Chem. Soc.* **1998**, *120*, 4035−4036. (e) Reich, H. J.; Green, D. P.; Medina, M. A.; Goldenberg, W. S.; Gudmundsson, B. Ö.; Dykstra, R. R.; Phillips, N. H. *J. Am. Chem. Soc.* **1998**, *120*, 7201−7210. (f) Reich, H. J.; Kulicke, K. J. *J. Am. Chem. Soc.* **1996**, *118*, 273−274. (g) Sikorski, W. H.; Sanders, A. W.; Reich, H. J. *Magn. Reson. Chem.* **1998**, *36*, S118−S124. (h) Sanders, A. W.; Reich, H. J., unpublished results. (i) Line-shape simulations were performed with the computer program WINDNMR: Reich, H. J. *J. Chem. Educ. Software* **1996**, *3D*, 2. (j) Reich, H. J.; Borst, J. P.; Dykstra, R. R.; Green, D. P. *J. Am. Chem. Soc.* **1993**, *115*, 8728−8741.

(16) Oakes, F. T.; Sebastian, J. F. *J. Organomet. Chem.* **1978**, *159*, 363−371.

(17) (a) Kalbarczyk-Bidelska, E.; Pasynkiewicz, S. *J. Organomet. Chem.* **1991**, *417*, 1−8. (b) Schumann, H.; Hartmann, U.; Wasserman, W.; Dietrich, A.; Görlitz, F. H.; Pohl, L.; Hostalek, M. *Chem. Ber.* **1990**, *123*, 2093−2100. (c) Atwood, J. L.; Berry, D. E.; Stobart, S. R.; Zaworotko, M. J. *Inorg. Chem.* **1983**, *22*, 3480−3482.

(18) Hope, H.; Power, P. P. *J. Am. Chem. Soc.* **1983**, *105*, 5320−5324.

(19) (a) Setzer, W. N.; Schleyer, P. v. R. *Adv. Organomet. Chem.* **1985**, *24*, 353−451. (b) Bauer, W.; Winchester, W. R.; Schleyer, P. v. R. *Organometallics* **1987**, *6*, 2371−2379.

(20) (a) The $^{1}J(^{13}C-^{7}Li)$ coupling is typically on the order of 10−14 Hz in tetramers, 20 Hz in dimers, and 40 Hz in monomers.[19b]

(21) Mahler, H.; Braun, M. *Chem. Ber.* **1991**, *124*, 1379−1395.

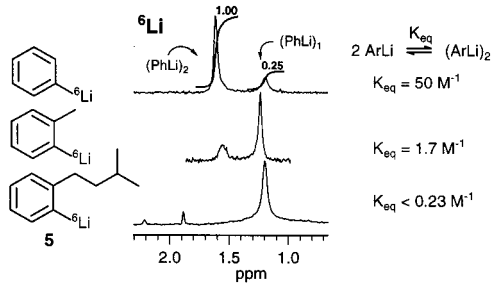

Figure 1. ^{6}Li NMR spectra of PhLi (0.2 M, 4:1 THF/Et_2O, −130 °C), *o*-TolLi (0.16 M, 4:1 THF/Et_2O, −125 °C), and **5** (0.11 M, 3:2 THF/Et_2O, −126 °C). The K_{eq} values are not strictly comparable because of small differences in the solvent composition and temperature.

Scheme 1. Synthesis of ^{15}N-Enriched 2-Trimethylstannyl-*N*,*N*-diethylbenzylamine

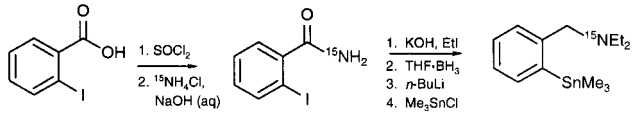

the mixture to equilibrate with HMPA and quenching with trimethylbromostannane. The pure lithium reagent was then formed by Sn−Li exchange with *n*-BuLi. Compounds **2**[22] and **3** could not be cleanly prepared by ortho metalation, and thus were prepared from the *o*-trimethylstannylbenzenes. These were available by reaction of 2-bromobenzyl bromide with the appropriate secondary amine, conversion to the lithium reagents by Li/Br exchange, followed by stannylation. The bromo compounds were not used directly to prepare lithium reagents for spectroscopic studies because of interference from LiBr (if *t*-BuLi was used) or 1-bromobutane (if *n*- or *s*-BuLi was used). To facilitate NMR studies, the ^{6}Li-enriched isotopomers of all compounds were prepared.[13b] The ^{15}N-enriched isotopomers of **1**, **2**, and **4** were prepared from the *o*-halobenzoic acids as exemplified in Scheme 1 for the precursor of **2**.

NMR studies were performed in mixtures of THF, diethyl ether, 2,5-dimethyltetrahydrofuran, and/or dimethyl ether to allow NMR studies at temperatures as low as −155 °C. Dimethyl ether is slightly less strongly solvating than THF; ether is much less so.

Model Compounds. Before discussing the results with the chelated compounds **1**−**4**, we briefly discuss some model systems. Phenyllithium has been extensively studied, both in solution[13c,15e,19b,23,24a] and in the solid state.[18,25−27] It exists as a mixture of monomer and dimer, with a K_{eq} for association of 30−40 M^{-1} in THF at −110 °C[15e,23a] and 50 M^{-1} in 4:1 THF/ether at −130 °C. *o*-Tolyllithium is slightly less associated, with K_{eq} = 1.7 M^{-1} in 4:1 THF/ether at −125 °C (Figure 1). A system which better models the steric effect of an ortho-alkyl substituent, 2-isoamylphenyllithium (**5**), is monomeric within the limits of detection. The small signal at δ 1.9 in the ^{6}Li NMR

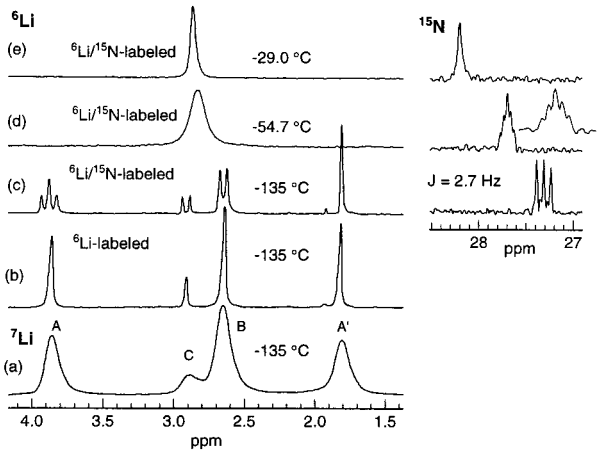

Figure 2. (a) 139.96 MHz ^{7}Li and (b−e) 52.98 MHz ^{6}Li and ^{15}N NMR spectra of natural abundance as well as ^{15}N- and/or ^{6}Li-labeled **1** in 3:2:1 THF/Me_2O/Et_2O at the indicated temperatures.

Scheme 2. Proposed Structures of the Dimers of **1**

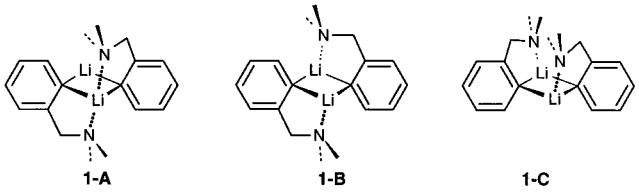

spectrum of **5** is the only signal which could conceivably be assigned to the dimer. It is 5% of the area of the monomer peak, so the compound is >95% monomeric, and the dimer association constant is <0.23 M^{-1}. Like PhLi, **5** complexes relatively weakly with TMEDA but quantitatively with PMDTA (>99% complex at 1 equiv in 3:2 THF/ether),[28] so the failure of some of the chelated compounds to complex effectively cannot be ascribed to steric effects of an ortho substituent. In fact, qualitatively the association equilibrium for PMDTA and **5** is even higher than that for PhLi, probably the result of the presence of more dimer in solutions of PhLi.[15e]

Solution Structures of the Chelated Organolithium Reagents. Figure 2 shows ^{7}Li, ^{6}Li, and ^{15}N NMR spectra of a sample of **1**. At low temperatures, four signals (which coalesced to one peak above −100 °C, Figure 2c−e) were observed in the Li NMR spectra. The ratio of the signals was concentration independent, so they do not correspond to different aggregates. The signals marked A and A′ were always present in a 1:1 ratio. One of them became a triplet in the ^{15}N and ^{6}Li doubly labeled compound (Figure 2c) and was thus coupled to two ^{15}N nuclei.[24b,29,30] The other remained a singlet with no coupling to ^{15}N. For the isomers **B** and **C**, each Li was coupled to one nitrogen. The ^{15}N signals in the ^{6}Li−^{15}N double-labeled isotopomer were not resolved. Rather, the spectrum showed a prominent 1:1:1 triplet (presumably isomers **A** and **B** superimposed) as well as a slightly offset smaller triplet (isomer **C**) from coupling of each nitrogen to a single ^{6}Li. These data strongly support the assignment to **A** and the **B**/**C** pair, as shown in Scheme 2, but do not allow the **B** and **C** isomers to be distinguished.[31] We will refer to these as shown in Scheme 2

(22) Longoni, G.; Fantucci, P.; Chini, P.; Canziani, F. *J. Organomet. Chem.* **1972**, *39*, 413−425.
(23) (a) Bauer, W.; Seebach, D. *Helv. Chim. Acta* **1984**, *67*, 1972−1988. (b) Jackman, L. M.; Scarmoutzos, L. M.; DeBrosse, C. W. *J. Am. Chem. Soc.* **1987**, *109*, 5355−5361.
(24) (a) Eppers, O.; Günther, H. *Helv. Chim. Acta* **1992**, *75*, 2553−2562. (b) Huls, D.; Günther, H.; van Koten, G.; Wijkens, P.; Jastrzebski, J. T. B. H. *Angew. Chem., Int. Ed. Engl.* **1997**, *36*, 2629−2631.
(25) Berger, S.; Fleischer, U.; Geletneky, C.; Lohrenz, J. C. W. *Chem. Ber.* **1995**, *128*, 1183−1186.
(26) (a) Schümann, U.; Kopf, J.; Weiss, E. *Angew. Chem.* **1985**, *97*, 222; *Angew. Chem., Int. Ed. Engl.* **1985**, *24*, 215−216. (b) Thoennes, D.; Weiss, E. *Chem. Ber.* **1978**, *111*, 3157−3161.
(27) Dinnebier R. E.; Behrens, U.; Olbrich, F. *J. Am. Chem. Soc.* **1998**, *120*, 1430−1433.
(28) Spectra and data in Supporting Information.
(29) Sato, D.; Kawasaki, H.; Shimada, I.; Arata, Y.; Okamura, K.; Date, T.; Koga, K. *J. Am. Chem. Soc.* **1992**, *114*, 761−763.
(30) Waldmüller, D.; Kotsatos, B.; Nichols, M. A.; Williard, P. G. *J. Am. Chem. Soc.* **1997**, *119*, 5479−5480.
(31) Chelation isomers of a similar type have been identified for tetrameric 3-dimethylaminopropyllithium,[4d] dimeric 1,1-bis(dimethylaminomethyl)-2-lithiopropane,[4d] and 3-lithio-1,5-dimethoxypentane.[4c]

Table 1. ^{13}C Chemical Shifts of ArLi

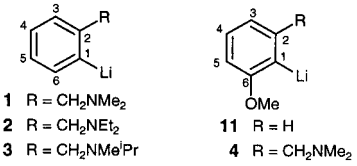

	solvent	temp (°C)	δ C-1 (J_{CLi})	δ C-2	δ C-3	δ C-4	δ C-5	δ C-6	δ NMe_2	δ CH_2N	δ OMe	ref
$(PhLi)_4$	Et_2O	−106	174.0 (5.1)	143.8	126.3	125.5	126.3	143.8				15e
$(PhLi)_2$	THF	−111	188.2 (7.9)	144.5	124.6	123.0	124.6	144.5				15e
$(PhLi)_1$	THF	−111	196.4 (15.3)	143.2	124.1	120.7	124.1	143.2				15e
$(\mathbf{5})_1$	*a*	−126	195.2 (15.2)	153.6	121.1* [g]	121.6*	123.4*	142.5	–	–		
1-A	*b*	−132	188.8 (7.0)	152.2	123.9*	123.4*	125.0	143.5	44.0, 48.1	72.0		
1-B	*b*	−132	188.4 (7.0)	151.9	123.9	123.5	125.1	143.2	43.0, 47.3	71.8		
1-C	*b*	−132	*c*	151.2	124.0	123.2	125.3	143.0	*c*	72.4		
2-B	Et_2O	−120	188.5 (7.8)	151.9	123.9*	124.2*	125.4	143.7	*c*	72.6		
3	*d*	−125	188.4 (−)	151.4	123.1*	123.7*	125.5	143.3	*c*	*c*		
$(\mathbf{4})_1$	*d*	−127	165.4 (12.6)	151.5	117.0	123.2	104.9	168.4	45.5	71.5	53.9	
$(\mathbf{4})_2$	*d*	−127	172.0 (6.3[e])	151.4	120.0	124.4	103.5	168.8	45.8f	70.5	54.3	
$(\mathbf{11})_1$·PMDTA	PhMe	−63	175.6 (13.6)	142.8	121.5	129.0	106.4	169.8			53.9	32
$(\mathbf{11})_2$·TMEDA	PhMe	−60	171.1 (6.8)	143.7	121.8	128.4	106.1	169.7			54.0	32
$(\mathbf{11})_4$	PhMe	−35	155.9 (5.1)	141.6	122.3	129.1	107.0	169.8			54.1	32

[a] 45:25:30 THF/Me_2O/ether. [b] 3:2:1 THF/Me_2O/ether. [c] Signal not found. [d] 3:2 THF/ether. [e] Splitting not resolved; coupling estimated from simulated spectra. [f] Signal is broad at −127 °C, probably due to intramolecular exchange. [g] Assignments were not made for chemical shifts marked with asterisks.

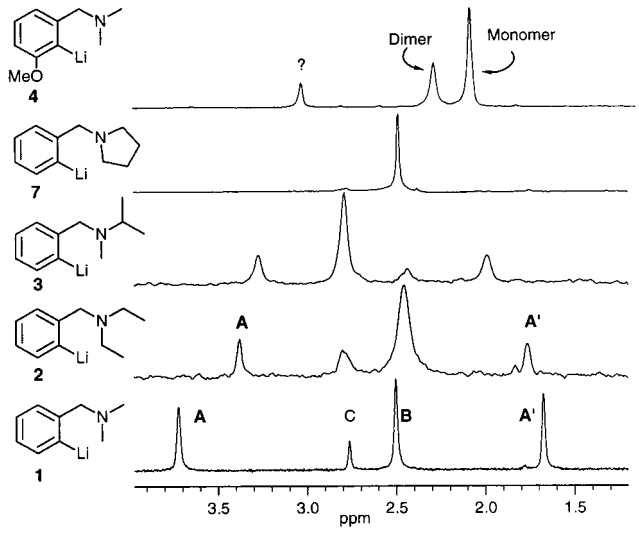

Figure 3. Li NMR spectra of ∼0.16 M ArLi: **1** (^6Li, −136 °C, 3:2:1 THF/Me_2O/ether); **2** and **7** (^6Li, −120 °C, 3:2 THF/ether); **3** (^7Li, −120 °C, 3:2 THF/ether), **4** (^6Li, −130 °C, 3:2 THF/ether).

with the NMR signal assignments as in Figures 2 and 3, but we will defer discussion of the **B**/**C** distinction until after we have considered the spectroscopic properties of all the compounds in more detail.

Other spectroscopic data supported the assignments for **1** made above. The ^{13}C NMR spectra showed three sets of signals in the same ratio as the Li signals for **A**, **B**, and **C** (Table 1; the minor isomer **C** was not resolved for all of the carbons). The NMe_2 ^{13}C signals were diastereotopic, with a $\Delta\delta$ of ca. 4 ppm. Two distinct C−Li signals were observed at −135 °C, each a 1:2:3:2:1 quintet with $J_{^{13}C-^6Li} = 7.0$ Hz from ^{13}C coupled to two ^6Li nuclei, consistent with a four-center dimer structure.[28] The signals coalesced to a single quintet by −60 °C.

The ^6Li NMR spectra of all of the ortho metalated aryllithiums are shown in Figure 3. The assignments for **2** were confirmed by NMR studies of the $^{15}N-^6Li$ doubly labeled compound (Figure 4). For **3**, the chemical shifts showed sufficient consistency that we have assigned those similarly. The relative amounts of the **A**, **B**, and **C** isomers differed substantially as

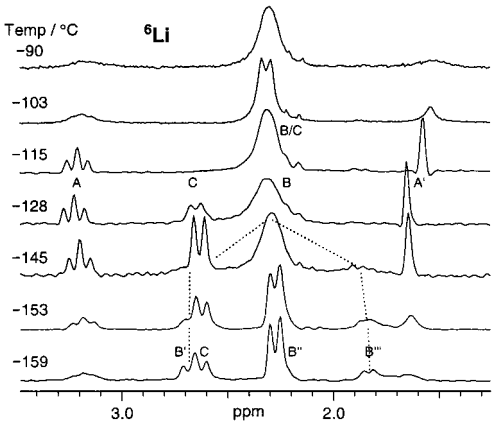

Figure 4. Variable-temperature ^6Li NMR spectra of ∼0.08 M ^6Li/^{15}N-labeled **2** in 45:30:25 THF/Et_2O/Me_2O.

the N-substituents were changed, with **A** as the major isomer for **1**, **B** as the major isomer for **2** and **7**, and **C** as the major isomer for **3**.

Compound **4** is qualitatively different from the others. The *o*-methoxy substituent has destabilized the dimer, so that now there are approximately equal amounts of monomer and dimer. This assignment was confirmed by a plot of log [monomer] vs log [dimer], which had a slope of 2.1.[28] The ^{15}N isotopomer showed Li−N coupling to a single nitrogen for both signals, so the monomer and dimer are both chelated, and the dimer is of the **B**/**C** type (Figure 5).

The ^{13}C chemical shifts of the lithium reagents are presented in Table 1, together with the shifts of the tetramer, dimer, and monomer of phenyllithium[15e] and 2-methoxyphenyllithium (**11**).[32] Particularly the C−Li carbon (C-1) chemical shift of 186−189 ppm is strongly supportive of dimeric structures for **1**−**3** in solution, since in related monomers and tetramers this carbon appears at ca. 195 and 175 ppm, respectively.[15e,33] This assignment is supported by the C−Li coupling observed (1:2:

(32) Harder, S.; Boersma, J.; Brandsma, L.; van Mier, G. P. M.; Kanters, J. A. *J. Organomet. Chem.* **1989**, *364*, 1−16. Boersma, J., private communication. We thank Prof. Boersma for providing these chemical shifts.

(33) Bertz, S. H.; Dabbagh, G.; He, X.; Power, P. P. *J. Am. Chem. Soc.* **1993**, *115*, 11640−11641.

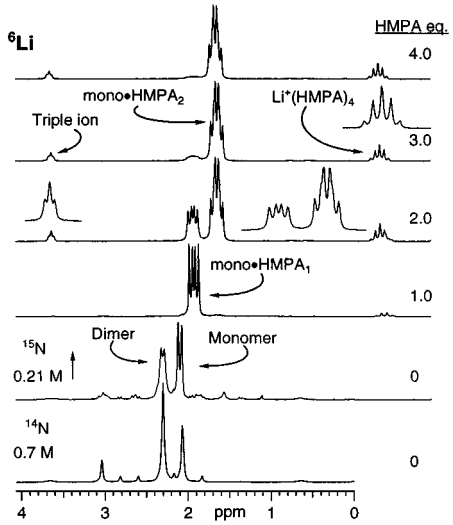

Figure 5. HMPA titration of 0.21 M ^{6}Li/^{15}N-labeled **4** in 3:2 THF/ether at −127 °C.

Scheme 3. Key Structural Features of the **A**, **B**, and **C** Dimers of **1** (S = solvent)

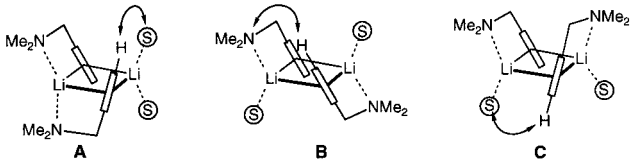

3:2:1 quintet in the ^{6}Li compounds). The ^{13}C chemical shifts of the methoxy analogue of **1**, compound **4**, are more properly compared to those of **11**. The available data are for the tetrameric toluene solvate, the dimeric TMEDA complex, and the monomeric PMDTA complex.[32] Like PhLi, **11** shows a progression of downfield shifts for the C−Li carbon between tetramer, dimer, and monomer. Compound **4** is anomalous, with the dimer shift downfield of the monomer by 6.6 ppm. Perhaps the *o*-methoxy substituent is hindering solvation of the dimer (see structures **A** and **C** in Scheme 3), resulting in an abnormally strongly polarized C−Li bond in the dimer, and consequently a larger paramagnetic shift.[13c,25]

Variable-Temperature NMR Studies. All of the lithium reagents show dynamic effects in their variable-temperature NMR spectra. These are of two types: intraaggregate processes involving the chelating groups (e.g., interconversion of **A**/**B**/**C** isomers) and interaggregate exchange (dimer−tetramer, dimer−trimer, and/or dimer−monomer exchange, detected mainly by loss of Li coupling to ^{13}C or ^{15}N).

(i) Intraaggregate Exchange. Above −135 °C, the **A**, **B**, and **C** isomers of **1** undergo a dynamic process detectable by ^{6}Li, ^{7}Li, ^{13}C, and ^{15}N NMR spectroscopy. Figure 6 shows that the four signals in the ^{6}Li NMR spectrum coalesce to a single peak between −122 and −88 °C. There are several discrete molecular processes which might be responsible for these changes:[4c,d]

(1) Dissociation of the **B** and **C** isomers to monomers and recombination. This would interconvert isomers **B** and **C** and cause loss of C−Li coupling. Isomer **A** cannot directly fragment to two chelated monomers but would have to isomerize to **B** first.

(2) Decoordination of both amino groups and ring rotation. This would interconvert all signals.

(3) Decoordination of one of the dimethylamino groups.

(3-a) Ring rotation around the C^1−C$^{1'}$ axis faster than recoordination. This would interconvert any isomer to any of the others but would not directly interconvert the A and A′ signals.

(3-b) Ring rotation slower than recoordination. This would allow interconversion of **A** with **B**, but neither **A** nor **B** could be interconverted with **C** by this process alone.

(4) Rotation of one phenyl group about the C^1−C$^{1'}$ axis without Li−N decoordination. This mode of isomerization, which requires little more than dissociation of a solvent molecule, would allow only interconversion of isomers **B** and **C**.

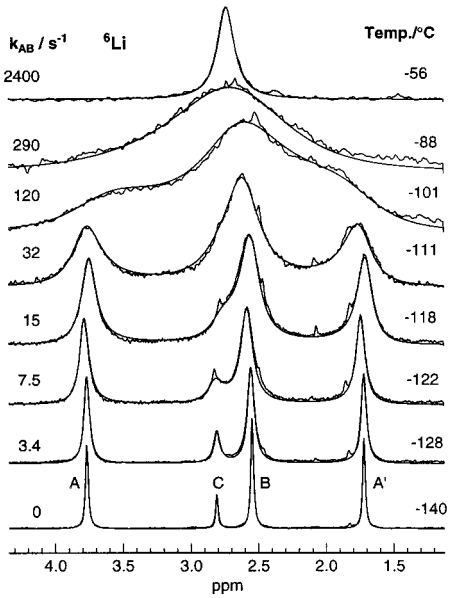

Figure 6. Variable-temperature 52.98 MHz ^{6}Li NMR study of **1** in 3:2:1 THF/Me_2O/Et_2O. The smooth lines are simulations using the exchange matrix of Figure 7 with the k_{AB} rates constants shown. We used k_{AC}/k_{AB} = 0.12 and k_{BC}/k_{AB} = 0.2, but because of the low population of **C** (10−11%) these rate constants have large errors. The k_{AB} rate constants shown give $\Delta H^{\ddagger}$ = 5.3 kcal/mol and $\Delta S^{\ddagger}$ = −18 eu.

Mechanism (1) can be ruled out on the basis of several kinds of NMR data. The C−Li coupling for C^1 is not lost until temperatures above −35 °C (vide infra), an observation also made by van Koten and co-workers for a THF/toluene solution of **6**.[14a] In the ^{15}N NMR study shown in Figure 2d,e, the ^{6}Li signals of **1**-**A**, **1**-**B**, and **1**-**C** have coalesced to a broad singlet at −55 °C, but the ^{15}N signal, which was a 1:1:1 triplet at low temperature, is now a 1:2:3:2:1 quintet, characteristic of a nitrogen equally coupled to two ^{6}Li nuclei. The dimethylamino groups are rapidly exchanging between all sites, but dissociation to monomers or association to tetramers is slow on the NMR time scale. At −29 °C, ^{6}Li−^{15}N coupling is lost, so intermolecular exchange has now become fast, and process (1) is occurring.

Mechanism (2) would allow all four signals to interconvert with each other. The direct exchange between the A and A′ signals of **1**-**A** was ruled out by a ^{6}Li EXSY experiment.[34] At a mixing time of 0.05 s at −131 °C, cross-peaks were detected between the A/A′ signals and B signals of **1**, as well as between signals B and C. No cross-peaks were detected between the A and A′ signals, thus ruling out mechanism (2). Cross-peaks were also not detected between A and C, either because of the small size of the C signal or because of the slow rate of exchange between A/A′ and C.

(34) Perrin, C. L.; Dwyer, T. J. *Chem. Rev.* **1990**, *90*, 935−967.

	A	A′	B	C
A	ν_A-1/T_A -k_{AB}-k_{AC}	0	k_{AB}	k_{AC}
A′	0	ν_A′-1/$T_{A'}$ -k_{AB}-k_{AC}	k_{AB}	k_{AC}
B	$k_{BA}/2$	$k_{BA}/2$	ν_B-1/T_B -k_{BA}-k_{BC}	k_{BC}
C	$k_{CA}/2$	$k_{CA}/2$	k_{CB}	ν_C-1/T_C -k_{CA}-k_{CB}

$k_{BA} = k_{AB}$·pop(A+A′)/pop(B)
$k_{CA} = k_{AC}$·pop(A+A′)/pop(C)
$k_{CB} = k_{BC}$·pop(B)/pop(C)
At -118 °C:
A : B : C = 52 : 38 : 10
k_{AB} = 14 s^{-1}, k_{BA} = 20 s^{-1}
k_{AC} = 3.4 s^{-1}, k_{CA} = 17 s^{-1}
k_{BC} = 2.1 s^{-1}, k_{CB} = 7.7 s^{-1}

Figure 7. Exchange matrix for the **A**/**B**/**C** exchange of **1**, with results given at one temperature ($1/T_X = \pi\nu_{1/2}$, the intrinsic line width, $\nu_{1/2}$ = line width at half-height).

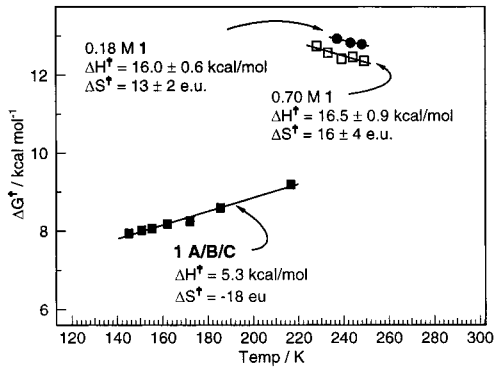

Figure 8. Temperature dependence of DNMR exchange rates: the **A**/**B**/**C** interconversion of **1** in 3:2:1 THF/Me_2O/Et_2O solution, and the loss of C−Li coupling in **1** (two concentrations) in 3:2 THF/ether.

The exclusive operation of either (3-b) or (4) can be ruled out for **1** because each would require selective coalescences: for (3-b) only between **B** and **C** without involving **A**, and for (4) only between **A** and **B** without involving **C**. Thus, if one of these processes is occurring, it cannot be the only one. We are thus left with (3-a) or both (3-b) and (4) operating at comparable rates.

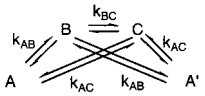

A four-spin DNMR simulation of the variable-temperature NMR spectra in Figure 6 was performed using the exchange matrix in Figure 7.[15i,35] Three independent rate constants were optimized, k_{AB}, k_{BC}, and k_{AC}. A satisfactory line fit could be achieved only when no exchange between the A and A′ signals was permitted, confirming that random exchanges are not involved (mechanisms (1) and (2)).

The changes in line shape are dominated by the **A**/**B** exchange, which is reasonable since these are the major isomers and this process requires only minimal rearrangement of the structure (movement of a dimethylamino group from one lithium to another). The **B**/**C** exchange appears to be slower than the **A**/**B** exchange but cannot be defined very accurately because of the small intensity of the **C** signal, its nearness to the signal for **B**, and the presence of a small impurity on top of the signal for **C**. This is in contrast to **2**, which shows k_{BC} larger than k_{AB} or k_{AC} (vide infra). The spectra can be adequately simulated with a small or no A/C exchange.

The temperature dependence of k_{AB} is presented in Figure 8. The substantial negative entropy of activation for the process (−18 eu) suggests an associative process for the isomerization, e.g., a mechanism in which a solvent molecule coordinates to one of the lithiums, followed by expulsion of the chelating group.

The diethylamino analogue **2** also showed the **A**, **B**, and **C** isomers (Figure 3), but the dynamic processes were more complex than for **1**. Relevant ^{6}Li NMR spectra are shown in Figure 4 for the ^{6}Li/^{15}N-labeled isotopomer. The −128 °C spectrum was very similar to the −135 °C spectrum for **1** in Figure 2, except that the signal assigned to **2-B** was quite broad. Lowering the temperature to −159 °C caused decoalescence of this signal into three doublets (labeled B′, B″, and B‴). No similar changes were seen for **1**. A plausible assignment for this dynamic process, which has an activation energy of around 6.5 kcal/mol, is a restricted rotation around the *N*-ethyl groups.[36] If this is correct, it supports the isomer assignment we have made to **B**, which features a close approach of the diethylamino group to the ortho proton of the other aryl ring (Scheme 3). The A and A′ signals also broaden substantially below −145 °C, and there may be an incipient decoalescence for these signals as well.

As the temperature was raised above −128 °C, another interesting phenomenon was observed. The signals of **2-B** and **2-C** coalesced and at −103 °C formed an ^{15}N coupled doublet. In contrast to the behavior of **1**, the **2-B** and **2-C** isomers are substantially more labile than the **2-A** isomer. Process (4), rotation around the $C^1-C^{1'}$ axis to interconvert **B** and **C** without involving **A**, is faster than the others. At −103 °C and higher, **2-A** begins to exchange with the coalesced **2-B**/**C** signals, as for **1**.

(ii) Interaggregate Exchange. Aggregate exchange can be addressed using the ^{13}C NMR signal of the C−^{6}Li carbon.[13d] This carbon appears as one or more 1:2:3:2:1 quintets at low temperature, which coalesce first to a single quintet (**A**/**B**/**C** exchange), and then to a singlet at higher temperatures, signaling the onset of interaggregate exchange.

The loss of C−Li coupling can occur by a number of mechanisms. For example:

(1) An associative process in which two dimers form a tetramer.

(2) An associative process in which a low steady-state concentration of monomers (or an adventitious Li−X salt) reacts with dimers to form transient trimers (or mixed trimers).

(3) A dissociation of dimers to monomers.

(4) A process in which a four-center dimer isomerizes to a triple ion ($Ar-Li^- - Ar\ Li^+$)[15d] followed by rapid intermolecular exchange of the free lithium cation.

Associative mechanisms (1) and (2) would show concentration-dependent rates, first-order increase for the tetramer mechanism, and half-order for the trimer mechanism. Mechanisms (3) and probably also (4) would give concentration-independent rates. We have determined the concentration dependence of the exchange rate for **1**. Experiments were performed on two samples differing in concentration by a factor of 4 (0.7 and 0.18 M) in 3:2 THF/ether solvent.

Simulations were performed using the exchange matrix of Figure 9,[15i] which corresponds to a random exchange mechanism. The exchange matrix was identical to one developed for a tetramer exchange mechanism[37] and differs only by a scaling factor of 1.5 for a trimer exchange mechanism. In the random and tetramer mechanism, 2/3 of encounters lead to exchange,

(35) Johnson, C. S., Jr. *Adv. Magn. Reson.* **1965**, *1*, 33−102. Johnson, C. S., Jr.; Moreland, C. G. *J. Chem. Educ.* **1973**, *50*, 477−483.

(36) Barriers on the order of 6 kcal/mol have been measured for rotation/inversion processes in methylethylisopropylamine: Reny, J.; Wang, C. Y.; Bushweller, C. H.; Anderson, W. G. *Tetrahedron Lett.* **1975**, 503−506.

(37) We thank Prof. Gideon Fraenkel for developing the exchange matrix for the exchange via tetramers.

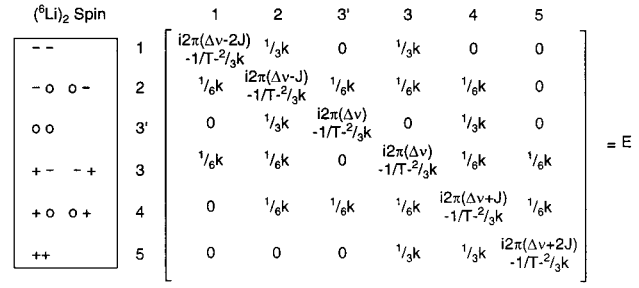

Figure 9. Exchange matrix for the random exchange of the 1:2:3:2:1 quintet of ^{13}C coupled to two ^{6}Li nuclei (k = rate constant for swapping of a lithium nucleus, $1/T = \pi\nu_{1/2}$, line width in the absence of exchange).

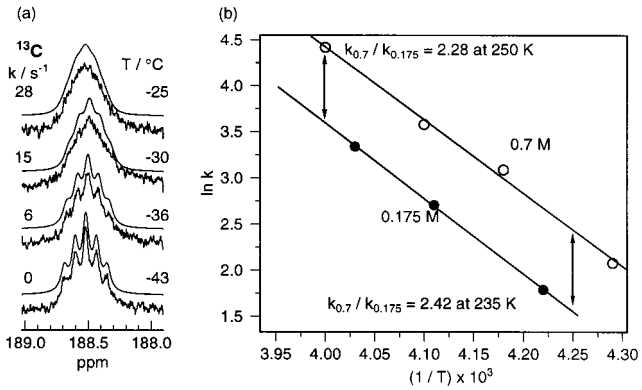

Figure 10. (a) Selected experimental and simulated ^{13}C NMR spectra of the C−Li carbon of 0.175 M ^{6}Li-labeled **1** in 3:2 THF/ether. The simulated spectra (upper curve of each pair) were obtained using the exchange matrix of Figure 9. The rates (see Figure 8) gave $\Delta G^{\ddagger}_{-30}$ = 12.8 kcal/mol, $\Delta H^{\ddagger} = 16.0 \pm 0.6$ kcal/mol, $\Delta S^{\ddagger} = 13 \pm 2$ eu for **1**. (b) Arrhenius plot for the concentration dependence of the rate of interaggregate exchange of ^{6}Li enriched **1** in 3:2 THF/ether solvent determined by loss of C−Li coupling in ^{13}C NMR spectra.

while in the trimer mechanism only 4/9 of the encounters result in exchange of spins. The line shape of the coalescing 1:2:3:2:1 quintet of the dimer cannot be used to distinguish the exchange mechanisms. Rates are summarized in the graph of Figure 8. Activation energies ($\Delta G^{\ddagger}$) for loss of C−Li coupling were in the range of 12−13 kcal/mol (Figure 10).

The rate data obtained are shown as an Arrhenius plot in Figure 10. The sample with a factor of 4 higher concentration has rate constants a factor of 2.3 higher at −23 °C, and a factor of 2.4 higher at −38 °C. We conclude, therefore, that the process is associative; the numbers obtained fit best for the trimer mechanism (2), which predicts a factor of 2 rate increase for a factor 4 increase in concentration. Of course, a mixture of mechanisms (1) and (3) or (1) and (2) could also lead to the fractional order observed.

Effect of Cosolvents. (i) Effect of TMEDA and PMDTA. We have examined the effect of TMEDA on the solution structures of **1** and **5**.[28] A ^{6}Li and ^{15}N NMR study of the addition of TMEDA to doubly labeled **1** is shown in Figure 11. The characteristic signals of the **A**/**B**/**C** isomers were replaced by a single major pair of signals in a 1:1 ratio, one a singlet and the other a triplet from coupling to two ^{15}N nuclei. These changes can be unambiguously interpreted in terms of conversion to a 1:1 complex **1-A**·TMEDA. The dependence on concentration of TMEDA is first order (a plot of [**1-A**·TMEDA]/[**1-A**] vs [TMEDA] has a slope of 1.1), ruling out the alternative monodentate structure for the TMEDA complex of dimeric **6** in toluene proposed by van Koten and co-workers.[14a]

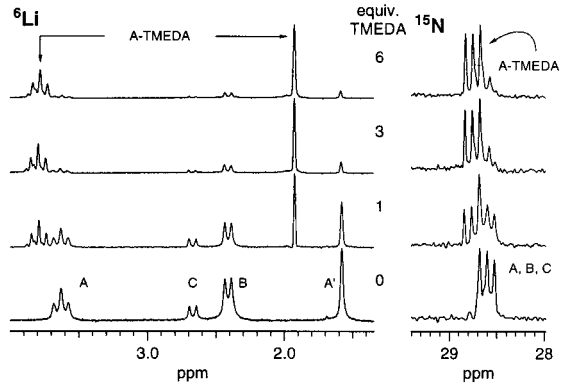

Figure 11. ^{6}Li NMR spectra ~0.16 M solution of ^{6}Li/^{15}N-labeled **1** in 3:2:1 THF/Me_2O/Et_2O at −135 °C as increments of TMEDA were added.

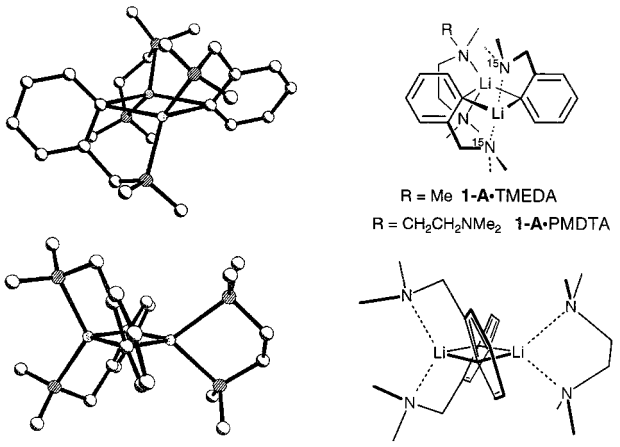

Figure 12. Two views of the X-ray crystal structure of **1-A**·TMEDA.

An equilibrium constant for the TMEDA association with **1** of $K_{eq} = 7.9\ M^{-1}$ was measured. Thus, TMEDA effectively displaces THF and/or dimethyl ether in this system.[38a] One comparison is as follows. When the molar ratio of TMEDA to THF is 1:36 (1 equiv of TMEDA), the ratio of the TMEDA and THF complexed species is 4:6. The actual effect is a factor of 2 higher since only about 50% of the material is the isomer **1-A** capable of complexing TMEDA in a bidentate fashion.

These conclusions are supported by the single-crystal X-ray structure (Figure 12) of the complex.[39] The structure shares many of the features found in other aryllithium dimers.[19a] The central four-membered ring has the typical small Li−C−Li angles (67.3 and 67.8°) and large C−Li−C angles (110 and 115°). The carbon−lithium bonds to the lithium chelated by TMEDA (2.36 and 2.35 Å) are longer than to the lithium coordinated intramolecularly (2.17 and 2.18 Å). This distortion is in the direction of incipient conversion to the triple ion **1-T**. The Li−N bond lengths are shorter for the chelated amines (2.06 and 2.06 Å) than for the TMEDA (2.15 and 2.19 Å). The constraint of intramolecular chelation also rotates the benzene rings from their normal orientation perpendicular to the central C_2Li_2 ring (as in the crystal structure of PhLi dimer[26b]) to an angle 24° off perpendicular (the angle between the planes of the two benzene rings is 48.9°).

The effect of PMDTA on **1** was almost identical to that of TMEDA (conversion to a complex **1-A**·PMDTA) in which the

(38) (a) In other systems TMEDA competes less well: Collum, D. B. *Acc. Chem. Res.* **1992**, *25*, 448−454. (b) Kim, Y.- J.; Bernstein, M. P.; Roth, A. S. G.; Romesberg, F. E.; Williard, P. G.; Fuller, D. J.; Harrison, A. T.; Collum D. B. *J. Org. Chem.* **1991**, *56*, 4435−4439.

(39) The X-ray data were archived with the preliminary communication.

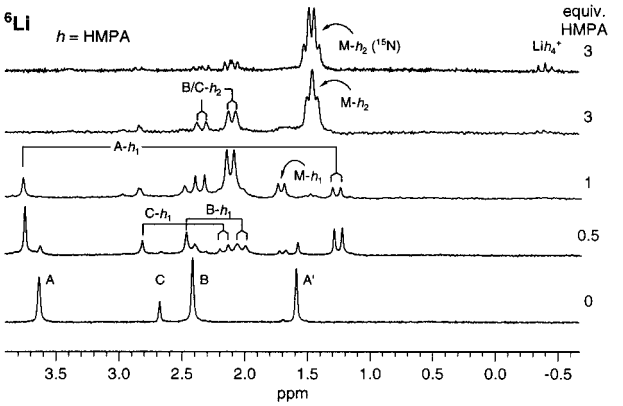

Figure 13. ^{6}Li NMR spectra of ~0.16 M ^{6}Li-labeled **1** in 3:2:1 THF/Me_2O/Et_2O at −135 °C. The top spectrum used ^{6}Li/^{15}N double-labeled material and also contained TMEDA (*h* = HMPA, M = monomer).

PMDTA coordinates in a bidentate fashion to the free lithium of **1-A**.[28,40a] The two Li peaks in the NMR spectrum of **1-A**·PMDTA were doubled due to stereoisomerism at the central nitrogen atom of the PMDTA. The association was significantly weaker, with a K_{eq} of 2.2 for the PMDTA complex vs 7.9 for TMEDA. There was one small signal at δ 2.2 in the ^{6}Li NMR spectra at 4 equiv of PMDTA (ca. 7% of total RLi equivalents) which could be the monomeric PMDTA complex, but a secure identification was not made (**5**·PMDTA has a Li signal at δ 2.1 in 3:2 THF/ether, and PhLi·PMDTA has a Li signal at δ 2).

(ii) Effect of HMPA. We have studied the changes in solution structure of **1**−**4** after addition of HMPA.[15j] We hoped this would provide qualitative information about the electrophilic nature of the different lithium environments in the various structures, as well as about the curiously strong dimerization of these chelated organolithium reagents. Figure 13 shows four spectra from an HMPA titration of **1** and the assignments we have made. At 0.5 equiv of HMPA, mono complexes of each of the chelation isomers **1-A**, **1-B**, and **1-C** were identified. The **A** and **C** isomers have about twice the HMPA affinity of the **B** isomer. Some mono-HMPA complex of **1** monomer (**1-M**) is also present (doublet at δ 1.7). At 1 equiv of HMPA, bis-solvates of the **B** and **C** isomers of **1** can be detected (one HMPA on each lithium), whereas no bis-HMPA complex of **A** was detected for this or the other compounds. This is reasonable, since the presence of one coordinated HMPA must greatly reduce the electrophilicity of the lithium.

Above 1 equiv of HMPA, there is a progressive increase in the fraction **1-M**·$(HMPA)_2$ complex (which shows an apparent quartet at δ 1.5 in the ^{15}N-labeled material due to approximately equal Li−P and Li−N coupling). Even at 3 equiv of HMPA, there are still significant amounts of the dimeric **B** and **C** bis-HMPA complexes. Thus, it is possible to break the dimers of **1**, although not quantitatively. At all equivalents of HMPA (and throughout this study for all compounds investigated which could form a five-membered-ring nitrogen chelate), we saw no indication of any species where the nitrogen was not fully chelated. At higher equivalents of HMPA, there are small signals for a separated $Li(HMPA)_4^+$ species at δ −0.4, which we believe are due to the triple ion **1-T**. The carbon-bound lithium of the triple ion can barely be detected at δ 3.35, so no clear identification of ^{6}Li−^{15}N coupling could be made in the double-labeled compound.

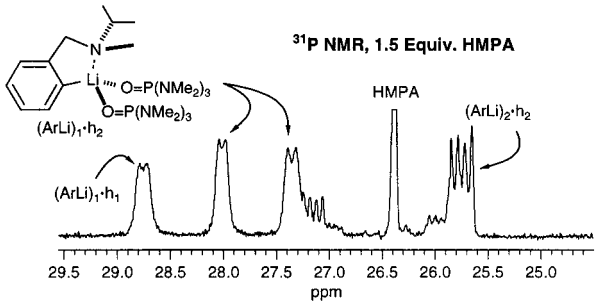

Figure 14. ^{31}P NMR spectra of 0.16 M **3** (natural abundance ^{7}Li) in 3:2 THF/ether at −120 °C with 1.5 equiv of HMPA (*h* = HMPA).

The behavior on treatment of **2** with HMPA[28] was similar to that observed for **1**, which showed an increase in the fraction of **1-C** for the mono-HMPA complexes (from 3:1 to 1:1 **B**:**C**), but then the bis-HMPA complexes favored **1-B** again by about a 2:1 margin. The ratio of isomers for **2**, which was 1:4:1 **A**:**B**:**C** in THF/ether, went to about 1:1:1 **A**:**B**:**C** for the mono-HMPA complexes and 0:3:1 **A**:**B**:**C** for the bis HMPA complexes.

Compound **3** showed another variation,[28] with the **3-C** mono- and bis-HMPA adducts forming predominantly and lesser amount of the **3-A** mono-HMPA complex. An interesting feature is that the ^{31}P signals of the monomeric bis-HMPA complexes are diastereotopic (Figure 14), confirming that at −120 °C decoordination and configurational inversion at both lithium and nitrogen are slow on the NMR time scale.[15f] The mono-HMPA complex of the monomer showed only a single HMPA signal, so the Li center is probably configurationally unstable as a result of fast dissociation of THF.

Compound **4** showed several interesting effects in its HMPA titration (Figure 5). In the early parts of the titration of the ^{15}N−^{6}Li-labeled compound, only the HMPA complex of the monomer was seen (δ 1.9, dd, J_{LiP} = 3.8, J_{LiN} = 2.2 Hz). Past 1 equiv of HMPA, free HMPA was observed, and bis-HMPA monomer signals appeared (δ 1.7, td, J_{LiP} = 2.9, J_{LiN} = 2.1 Hz). At no point was any dimer HMPA complex detected, in contrast to **1**, **2**, and **3**, in which both dimer and monomer mono- and bis-HMPA complexes are formed prominently. Exceptionally well resolved ^{13}C NMR spectra were obtained, and these allowed an examination of the effect of HMPA on C−Li δ and *J* values. The J_{C-Li} decreased in magnitude from 12.6 Hz for the THF-complexed monomer to 11.5 Hz for the mono-HMPA complex and 9.7 Hz for the bis-HMPA complex. The chemical shift moved progressively downfield from δ 165.4 to 167.9 and 171.5 ppm as HMPA was added. Both effects are consistent with C−Li bond-weakening as HMPA coordinates to Li. The most interesting signal, however, was the internal lithium of the triple ion at δ 3.6, a well-defined triplet, with $J^{6}_{Li-^{15}N}$ = 1.6 Hz. Thus, the triple ion adopts the predicted chelated structure **4-T**. Not even the presence of two strongly electron-donating Ph^- ligands on Li breaks the chelation.

X-ray Crystal Structure of 3. Figure 15 shows the single-crystal X-ray structure of the THF solvate of **3**. According to the assignment we have made, **3** is mostly isomer **C** in solution (the ratio **A**:**B**:**C** is 3:1:6, but the X-ray structure is that of the **B** isomer. Presumably the minor isomer crystallized, but we cannot rule out that the assignments of the signals in the Li NMR spectrum (Figure 3) are incorrect. The NMR spectra of **3** are potentially more complicated than those of **1**, **2**, and **4** because of the possibility of multiple isomers due to the asymmetric center at nitrogen (see Figure 14).

(40) (a) Vinyllithium also complexes with PMDTA as a dimer. It was not established whether the complexation of the PMDTA was bidentate or tridentate. Bauer, W.; Griesinger, C. *J. Am. Chem. Soc.* **1993**, *115*, 10871−10882. (b) Betz, J.; Hampel, F.; Bauer, W. *Org. Lett.* **2000**, *2*, 3805−3807.

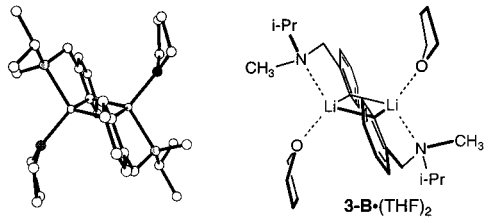

Figure 15. Single-crystal X-ray structure of **3-B**·$(THF)_2$.

The molecule occupies a crystallographic inversion center, and only one-half of the dimer is symmetry independent. The structure shows no unusual features compared to other aryllithiums, with normal N−Li (2.139(3) Å) and THF O−Li (1.939(3) Å) bond lengths. The two C−Li bonds are slightly different (2.186(3), 2.252(3) Å), with the shorter bond within the chelate ring (distortion in the direction of separating into two chelated monomers). The chelate bite angle C−Li−N is 98.62(11)°. The central C_2Li_2 ring has a C−Li−C angle of 113.05(11)° and a Li−C−Li angle of 66.95(11)°. The structure has several features of interest in the context of the **B**/**C** assignment. As found for the solid-state structure of **1-A**· TMEDA (Figure 12), chelation causes the phenyl rings to be rotated from their normal orientation perpendicular to the central C_2Li_2 ring by 20.8(1)°. The N-isopropyl groups are in what at first glance appears to be the more hindered position (near the ortho C−H of the other phenyl group). This choice of epimers at N may be solvation driven, since the other epimer would place the isopropyl groups in a position that would interfere with the coordinated THF molecules.

Distinguishing Isomers B and C. There are no unambiguous spectral features that allow us to distinguish the two signals for the **B** and **C** isomers of **1**−**3**. We have unsuccessfully attempted to identify them indirectly by examining the effect of bidentate cosolvents which might specifically complex isomer **C** by bridging the two Li atoms of the dimer (**12**). Such complexation,

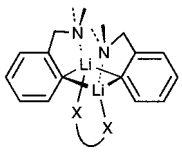

12

if the cosolvent was in fast exchange on the NMR time scale, would increase the fraction of **C** at equilibrium. Although such Li−Li′ bidentate coordination has not been directly detected in a dimer, similar coordination in a tetramer has been proposed to explain the kinetic effect of 1,4-bismethoxybutane on the addition of isopropyllithium to ethylene.[41] None of the cosolvents provided useful information for identifying the **B** and **C** isomers: TMEDA complexed the free lithium of **A** selectively (Figure 11); 1,3-dimethoxypropane and 1,4-(dimethylamino)-2-butyne gave no detectable changes in the **B**/**C** ratio; 1,4-bis-(methoxy)-2-butyne caused decomposition of **1**.

The assignment of the **B** and **C** structures as shown in Scheme 2 is supported by the single-crystal X-ray structure of **7**.[15h] This compound, which in our assignment is almost entirely the **B** isomer in THF solution (see Figure 3),[42] does have the **B** structure in the solid state. Unfortunately, the THF solvate of **3** also has the **B** isomer in the solid state, even though it appears to be mostly **C** in solution.

(41) Bartlett, P. D.; Goebel, C. V.; Weber, W. P. *J. Am. Chem. Soc.* **1969**, *91*, 7425−7434.

(42) Goldenberg, W. S. Ph. D Thesis, University of Wisconsin, Madison, 1999.

An examination of the single-crystal X-ray structures of **1-A**· TMEDA, **3-B**·$(THF)_2$, and **7-B**·$(THF)_2$ as well as MNDO- or PM3-minimized structures for the bis-THF solvates of **1-A**, **1-B**, and **1-C** shows that **A** and **C** have a substantial dihedral angle between the two phenyl rings (the rings are 24° off perpendicular in the X-ray structure of **1-A**·TMEDA), whereas **3-B** and **7-B** have the rings essentially coplanar by symmetry, but with this plane well off perpendicular to the C_2Li_2 plane (the angle is 32° in **3-B**·$(THF)_2$ and 38° in **7-B**·$(THF)_2$[15h]).[43] Consequently, in **A** and **C** there are steric repulsions between the aryl ortho hydrogen and one of the solvent molecules on Li, whereas in **B** the solvent location is very open (Scheme 3). On the other hand, **B** suffers from steric interactions between this same hydrogen and one of the N-alkyl groups of the other aryl ring. This provides a rationale for the curious observation that **2**, which is a 2:6:2 ratio of **A**:**B**:**C** in THF/ether, in 2,5-dimethyltetrahydrofuran/ether shows only a single isomer, with a chemical shift close to that of the peak assigned to the **2-B** isomer in THF/ether.[28] The larger solvent molecule can best be accommodated in the **2-B** structure. (An alternative explanation could be that **B** is favored in the less polar solvent because it is the only isomer with no dipole moment.) On the other hand, the molecule with the largest N-alkyl groups, **3**, is the only one in which isomer **C** is more populated than isomer **B** (Figure 3), because here **B** is maximally destabilized by the *o*-H/N−R interaction. Along the same lines, the compound with the smallest N-alkyl groups, **7**, shows only isomer **B**.[42]

Mixed Dimer of Phenyllithium and 1. One of the most puzzling aspects of the chemistry of these chelated aryllithium reagents is the strong propensity to form dimers under conditions where nonchelated analogues are significantly or entirely monomeric (Figure 1). We therefore examined mixtures of **1** with PhLi to see whether mixed dimers formed, and how they behaved in solution. The spectra in Figure 16 show that a mixed dimer **13** is prominently formed. The ^{13}C NMR signals of the phenyl portion are very close to those of PhLi dimer, and the remaining signals are very close to those of **1**.[28] The two lithiums of the dimer are nonequivalent, with Li chemical shifts nearly identical to PhLi dimer and **1-B**. As seen for the homodimer, amine decoordination is slow on the NMR time scale below −110 °C. The equilibrium constant for mixed dimer formation was $K_{eq} = 27$ at −131 °C. The statistical value would be $K_{eq} = 4$.

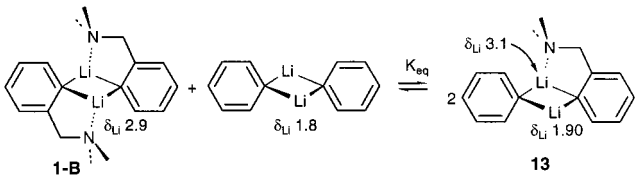

The favorable equilibrium constant for formation of the mixed dimer **13** allowed us to address the question of ring rotation about the $C^1-C^{1'}$ axis, discussed above in connection with the **1-A**/**B**/**C** interconversion. In a static structure, the two ortho and two meta carbons of the phenyl group in **13** should be diastereotopic. However, only a single set of signals could be detected for these carbons. Thus, either the ring rotation is still fast on the NMR time scale below −120 °C, or the signals are accidentally coincident.

A variable-temperature study of the mixed dimer (Figure 16) gave a remarkable series of spectra. A sequence of coalescences

(43) Even larger distortions toward coplanarity of the central C_2Li_2 and aryl rings in dimers have been observed for 8-(dimethylamino)-1-naphthyllithium.[14d] and 8-methoxy-1-naphthyllithium.[40b]

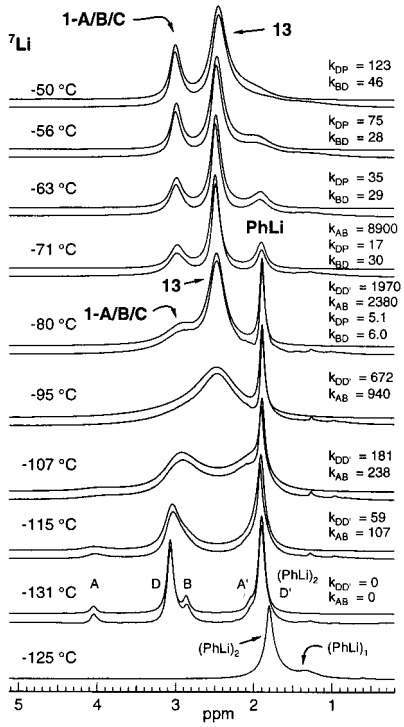

Figure 16. Variable-temperature ^{7}Li NMR study of a 1:1 mixture of **1** and PhLi in 4:2:1 Me_2O/THF/Et_2O. At each temperature, the lower curve is the experimental spectrum and the upper the simulation. The bottom spectrum is PhLi in 4:1 THF/ether (D, D′ = mixed dimer **13**).

can be observed. Between −115 and −63 °C, the **1-A/B/C** isomers coalesce into a single peak at 3.0 ppm. At a very similar rate, the two lithium signals of **13** coalesce to a signal at 2.5 ppm. Not easily observable in this sample is the coalescence of PhLi monomer and dimer which occurs at −100 to −75 °C.[15e] At −71 °C, the three signals correspond to the rapidly equilibrating **1-A/B/C** isomers, the equilibrated **13** signal, and the average of PhLi monomer and dimer. Between −71 and −49 °C, PhLi begins to coalesce with the two signals of **13**, suggesting that **13** is now undergoing dissociation to monomers. At −49 °C, the **1-A/B/C** and **13/PhLi** begin to average as **1** begins to exchange with the mixed dimer and the PhLi on the NMR time scale.

A complete line shape analysis of this system is not feasible because there are too many variables (>25) to establish them realistically from the data available: eight chemical shifts (four for **1**, two for **13**, two for PhLi), eight T_1 values, and five independent populations for the lithium signals; and rate constants for interconversion of the **1-A/B/C** isomers, equilibration of the lithium signals of **13**, equilibration of PhLi with **13**, equilibration of **1** with **13**, and equilibration of PhLi dimer and monomer.

We have performed simulations with the following simplifying assumptions: (1) we have ignored **1-C** (the peak is small, hidden under the downfield mixed dimer peak D, and quickly coalesces with **1-B**) and used only one rate constant, k_{AB}, for the intraaggregate exchange of **1**; (2) the PhLi monomer signal and the exchange between PhLi dimer and monomer was ignored (since in this solvent mixture there is <20% monomer, this exchange causes only a small degree of broadening of $(PhLi)_2$ around −80 to −100 °C); (3) only the D signal of the mixed dimer **13** was allowed to exchange with **1-B** (direct dissociation of **1-A** would require simultaneous breaking of both C−Li and N−Li bonds), and only the D′ signal of the mixed dimer was allowed to exchange with PhLi dimer (these assumptions would be true if the exchange was dissociative); (4) all peaks were assumed to have the same natural line width, 12 Hz (except for PhLi dimer at −80 and −95 °C, for which the line widths were 7 and 9 Hz). This is reasonable since all are ArLi dimers, with similar rates of molecular motion.[23b] The line shapes were simulated using the exchange matrix of Figure 17.[15i] This simulation used four rate constants, k_{AB} (the exchange between **1-A** and **1-B**), $k_{DD'}$ (exchange between the two peaks of the mixed dimer), k_{BD} (the exchange between **1-B** and the D peak of the mixed dimer **13**), and $k_{D'P}$ (the rate of exchange between PhLi and the D′ peak of the mixed dimer).

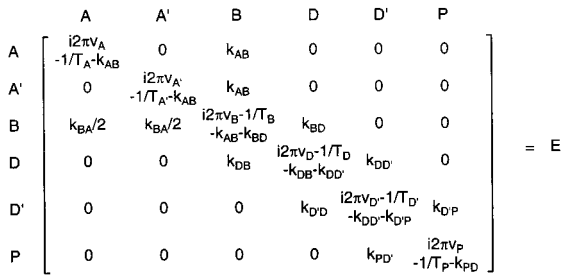

Figure 17. Exchange matrix for the interconversion of **1-A** (A and A′), **1-B** (B), **13** (D, D′), and PhLi (P) ($1/T_X = \pi\nu_{1/2}$, the intrinsic line width, $\nu_{1/2}$ = line width at half-height).

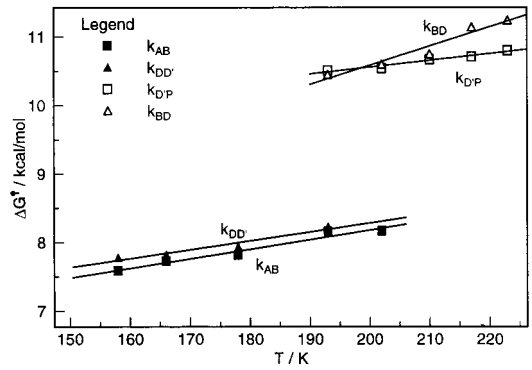

Figure 18. Eyring plot for the kinetic data determined from the variable-temperature NMR study of the mixed dimer (**13**) between PhLi and **1**. k_{AB}: $\Delta G^‡_{195} = 8.1$ kcal/mol, $\Delta H^‡ = 5.4 \pm 0.3$ kcal/mol, $\Delta S^‡ = -14 \pm 2$ eu. $k_{DD'}$: $\Delta G^‡_{195} = 8.2$ kcal/mol, $\Delta H^‡ = 5.7 \pm 0.4$ kcal/mol, $\Delta S^‡ = -13 \pm 2$ eu. k_{BD}: $\Delta G^‡_{195} = 10.5$ kcal/mol, $\Delta H^‡ = 5.0 \pm 0.8$ kcal/mol, $\Delta S^‡ = -28 \pm 4$ eu. $k_{D'P}$: $\Delta G^‡_{195} = 10.5$ kcal/mol, $\Delta H^‡ = 8.6 \pm 0.3$ kcal/mol, $\Delta S^‡ = -10 \pm 2$ eu. In the simulation, the rate constants k_{AB} and k_{BD} are interactive in the 190−200 K temperature range, so the activation parameters calculated for k_{BD}, which depends strongly on data points in this range, are suspect.

The high quality of the simulation (Figure 18) confirms that the rather complex changes in line shape have been correctly assigned and that the assumptions made are reasonable ones.

The two rate constants for intra-aggregate exchange, k_{AB} and $k_{DD'}$, are almost identical throughout the temperature range, and these rates are 100−500 times as fast as the exchange between **1-B** and the mixed dimer **13** (k_{BD}). The exchange between PhLi and **13** was marginally faster than exchange between **13** and **1-B**. Both of the interaggregate exchanges were just beginning to cause significant broadening at the highest temperature studied, so the rate data are less accurate than for the intramolecular exchanges. Thus, the unusually large $\Delta S^‡$ of −28 eu for k_{BD} is probably in error.

Chelation and Aggregation. The results obtained with the mixed dimer provide some quantitative information about, but no real understanding of, the strong tendency for these chelated compounds to aggregate (Scheme 4). Phenyllithium itself is

Scheme 4. Association Equilibria

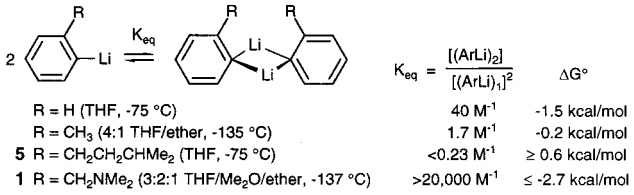

partially monomeric in THF solutions, ca. 1:1 monomer/dimer at 0.08 M,[15e,23a] and the model system **5** is entirely monomeric. Except for **4**, in which there are some additional steric and electronic effects, the chelated organolithium reagents are dimeric within the limits of detection. We estimate that <1.2% of monomer signal could be present (area of a small peak at δ 1.69 at −137 °C). Thus, assuming that the monomer signal is not hidden under one of the dimer signals, the dimer is at least 3 kcal/mol more stable when compared to the model dimer **5**.

The mixed dimer **13** is both thermodynamically (since it is formed in higher than statistical amount) and kinetically more stable toward dissociation than PhLi. The activation energy for aggregate exchange for **13** ($\Delta G^{\ddagger}_{-50} \geq 11.2$ kcal/mol) is almost 3 kcal/mol higher than the barrier for dissociation of PhLi dimers ($\Delta G^{\ddagger}_{-101} = 8.3$ kcal/mol).[15e] The homodimer **1** has a still higher barrier, with a $\Delta G^{\ddagger}_{-36}$ of 12.9 kcal/mol measured from the rate of collapse of the $^{13}C-^{6}Li$ coupling in the ^{13}C NMR spectra (Figure 10). This process is definitely bimolecular, so dissociation to monomer has a barrier higher than this. A second measure is provided by estimating the maximum broadening of the 1:2:3:2:1 quintet in the ^{6}Li NMR spectrum of $^{15}N-^{6}Li$ doubly labeled **1** at −55 °C (Figure 2d), which corresponds to a rate constant of ≤ 4.5 s^{-1} (DNMR simulation).[44] Since dissociation of the dimers would cause loss of Li−N coupling, $\Delta G^{\ddagger} \geq 12$ kcal/mol for this process.

The dimerization of organolithium reagents cancels the C−Li dipole, and this is presumably the major driving force promoting aggregation. Opposing effects are loss of solvation as well as steric repulsion between the carbanion and solvent ligands on lithium. Thus, either an increase in the C−Li dipole of the monomer or reduced steric effects might be responsible for the high tendency of these chelated compounds to aggregate. The smaller C−Li−N bite angle (90° in **1-A**·TMEDA[15a]) for a chelated group compared to the C−Li−(solv) angle of a nonchelated analogue could result in a larger dipole since there would be less cancellation of the C−Li and X−Li dipoles (where X is either the chelating N or the O of a solvent molecule). The smaller bite angle could also result in less steric resistance to dimerization. In addition, the N-chelating group may be a weaker donor than a molecule of THF which it replaces, which would also increase the C−Li dipole.

Some support for a more polar lithium environment in N-chelated compounds is provided by the observation that the monomeric amine-chelated organolithium reagents **14** and **16** showed a higher HMPA affinity than did nonchelated analogues **15** and **17** (Scheme 5). HMPA was added to a 1:1 mixture of **14** and **15**, and the concentration of the THF- and HMPA-complexed lithium reagents was measured by ^{31}P and ^{7}Li NMR spectroscopy. There was a significant preference for coordination of HMPA to the chelated compound **14**, corresponding to a free energy of 0.5 kcal/mol. The effect was larger for the analogue in which $PhMe_2Si$ replaced the PhS group (comparison of **16** and **17**), where $K_{eq} = 10$ and $\Delta\Delta G = -0.7$ kcal/mol.[28] The

(44) This rate constant was estimated from a DNMR simulation using the exchange matrix of Figure 9, with a natural line width of 0.1 Hz.

Scheme 5. HMPA Affinities

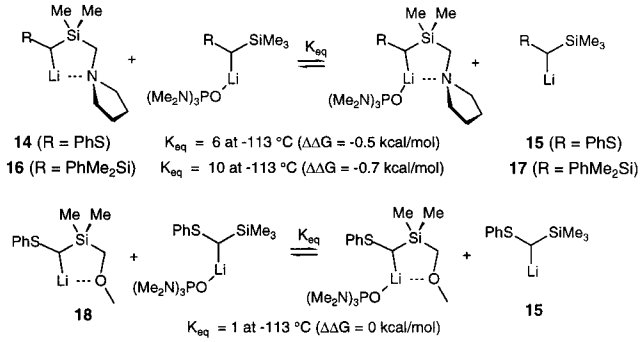

same experiment on the methoxy-chelated analogue **18** gave a $K_{eq} = 1$ ($\Delta\Delta G = 0$). These experiments imply that the steric effect of a tertiary amine chelating group is not overwhelming and that the amino group of the chelated compound **14** is a weaker donor than a solvated THF in **15** or the chelated oxygen in **18**. In other words, the lithium is more electrophilic and the C−Li bond is more strongly polarized in **14** and **16** than in model systems.

If the same effect is present in the amine-chelated aryllithium reagents, it provides at least a partial explanation for their tendency to dimerize, since dimerization cancels the C−Li dipole. There are some weak indications that the chelated lithiums in these aryllithium reagents are more electrophilic from examination of HMPA complexation to the **1**/PhLi mixed dimer.[28] HMPA showed a slightly higher affinity (3:2) for the N-chelated lithium (signal D, Figure 16) of the mixed dimer **13** than for the other one. On the other hand, the nonchelated lithium of **1-A** showed a higher affinity than the chelated lithium of the **1-B** and **1-C** isomers, which would imply the opposite effect. Unfortunately, one knows very little about steric effects and the ether solvation state of these compounds, so comparisons of this type provide little basis for understanding the aggregation state.

Summary. Three of the compounds with ortho dialkylaminomethyl groups investigated (**1**, **2**, and **3**) are strongly chelated and dimeric in solvents containing THF mixed with ether and/or dimethyl ether based on NMR spectroscopic studies of ^{6}Li- and ^{15}N-enriched compounds. The dimers exist as mixtures of three chelation isomers, which are in dynamic equilibrium with activation energies of ca. 8 kcal/mol (analogous to several chelated aliphatic organolithium reagent aggregates[4d]). Both TMEDA and PMDTA complex to **1** in a bidentate fashion, but neither cosolvent causes loss of chelation or significant dissociation to monomers. Not even HMPA causes dechelation, although a large excess causes almost complete cleavage of dimers to monomers.

A fourth compound with a methoxy ortho substituent (**4**) is also strongly chelated but is only partially dimeric, presumably for steric reasons. Addition of HMPA first causes complete deaggregation to HMPA-complexed monomer, and then a partial redimerization to form the bis-chelated triple ion **4-T**.

The most unusual aspect of the behavior of these compounds is the relatively high kinetic and thermodynamic stability of the dimers. It remains to be determined whether this is a general phenomenon, but oxygen-chelated analogues are also more dimeric than model systems.[15b] Some support for a hypothesis in which this effect is a consequence of a higher C−Li bond polarity was obtained. Interaggregate exchange of **1** has been shown to proceed by a mechanism involving association through trimers or tetramers and not by dissociation to monomers, yet another reflection of the high stability of the dimers.

Compound **1** forms a mixed dimer with PhLi, which also shows the features of high kinetic and thermodynamic stability in dissociation to monomers compared to nonchelated analogues. Thus, even a single chelating group stabilizes a dimeric structure.

Experimental Section

General. All reactions requiring a dry anoxic atmosphere were performed in glassware flame-dried or dried overnight in a 110 °C oven, sealed with septa, and flushed with N_2. Tetrahydrofuran (THF) and diethyl ether (ether) were freshly distilled under N_2 from sodium benzophenone ketyl. Dimethyl ether (Me_2O, bp −24.8 °C) was condensed from a pressurized gas cylinder into a graduated conical tube cooled to −78 °C, *n*-BuLi was added, and the dry Me_2O was passed by cannula into the desired vessel cooled to −78 °C. *N*,*N*,*N*′,*N*″-Tetramethylethylenediamine (TMEDA), *N*,*N*,*N*′,*N*″,*N*″-pentamethyldiethylenetriamine (PMDTA), and hexamethylphosphoric triamide (HMPA) were distilled from CaH_2 under reduced pressure (if required) and stored under N_2 over 4 Å molecular sieves. Common lithium reagents were handled by septum and syringe-based techniques and titrated against dry 1-propanol in THF with 1,10-phenanthroline as an indicator.[45] Et^{6}Li[38b] (from EtBr and ^{6}Li metal) and *n*-Bu^{6}Li[13b] (*n*-BuCl and ^{6}Li metal) were prepared by literature methods. All reported reaction temperatures are those of the cooling baths. Thin-layer chromatography (TLC) was conducted on silica gel 60 F_{254} plates and visualized by ultraviolet irradiation. Melting and boiling points are reported uncorrected. Kugelrohr distillation temperatures refer to the pot temperature. Mass spectra were obtained on a Kratos MS-80 spectrometer.

Routine NMR Spectroscopy. Routine ^{1}H and ^{13}C nuclear magnetic resonance (NMR) spectra were obtained on Bruker AC-300, AVANCE or AM-360 and AM-500 spectrometers. All spectra were acquired in $CDCl_3$ or C_6D_6, with tetramethylsilane (TMS, δ 0.00) as an internal reference for ^{1}H NMR and $CDCl_3$ (δ 77.0) or C_6D_6 (δ 128.0) for ^{13}C NMR spectra. Routine ^{119}Sn NMR spectra were obtained on a Bruker AM-360 spectrometer (unlocked) and were acquired in protio-THF, with tetramethylstannane (δ 0.00) as an internal reference.

Low-Temperature Multinuclear NMR Spectroscopy. All low-temperature multinuclear NMR experiments were conducted on a Bruker AVANCE-360 or AM-360 spectrometer equipped with a 10-mm wide-bore broadband probe at the following frequencies: 360.148 MHz (^{1}H), 90.556 MHz (^{13}C), 52.984 MHz (^{6}Li), 139.905 MHz (^{7}Li), and 145.785 MHz (^{31}P).

All spectra were taken of samples in a combination of the protio solvents THF, ether, and/or Me_2O with the spectrometer unlocked. ^{13}C NMR spectra were referenced internally to the C-2 carbon of THF (δ 67.96), the C-2 carbon of ether (δ 66.57), or Me_2O (δ 60.25). Lorentzian multiplication (LB) of 2−3 Hz was applied to ^{13}C NMR spectra. ^{6}Li and ^{7}Li NMR spectra were referenced externally to 0.3 M LiCl/MeOH (δ 0.00) or internally to $Li^+(HMPA)_4$ (δ −0.40). ^{31}P NMR spectra were referenced externally to 1.0 M PPh_3/THF (δ −6.00) or internally to free HMPA (δ 26.40). Probe temperatures were measured externally by ejecting the sample and inserting a thermocouple into the probe or internally with the ^{13}C chemical shift thermometer $(Me_3Si)_3CH$.[15g]

Benzamide-[^{15}N].[46] $^{15}NH_4Cl$ (98%, 0.5 g, 9.2 mmol) was dissolved in 7 mL of water in a one-neck round-bottom flask. The water was covered with a layer of benzene (1−2 mL), the flask was cooled in an ice bath, and to it was added (by pipet inserted through the benzene layer) a solution of NaOH (0.79 g, 19.7 mmol in 5 mL of water), followed immediately by benzoyl chloride (1.1 mL, 9.4 mmol) in 40 mL of benzene. The ice bath was removed, the flask fitted with a septum, and the solution stirred at room temperature for 1.5 h (precipitate of benzamide). The solution was cooled in ice, and the solid was filtered, washed with water and cold benzene, and allowed to air-dry to give 0.91 g of benzamide. A further 54 mg of benzamide (total yield of 86%) was obtained by extracting the solvent and rinsing the flask with CH_2Cl_2. The product was used without further purification. ^{1}H NMR ($CDCl_3$, 300 MHz): δ 6.25 (d, $^1J_{N-H}$ = 88.6 Hz, 2H), 7.41−7.57 (m, 3H), 7.8−7.85 (m, 2H). ^{13}C{^{1}H} NMR ($CDCl_3$, 75.45 MHz): δ 127.3 (*o*), 128.6 (*m*), 131.9 (*p*), 133.4 (*i*, $^2J_{C-N}$ = 8.3 Hz), 170.0 (C=O, $^1J_{C-N}$ = 15.3 Hz).

Benzylamine-[^{15}N]. $LiAlH_4$ (0.78, 20.6 mmol) was suspended in 35 mL of dry THF and cooled to 0 °C. [^{15}N]-Benzamide (0.84 g, 6.9 mmol) in 10 mL of THF was added dropwise to the stirred suspension. The mixture was refluxed for 12 h and slowly cooled to 0 °C, and then 1 mL of 15% NaOH and 4 mL of water were added. The mixture was stirred for several minutes and filtered, and the clear filtrate was dried (Na_2SO_4). The solvent was evaporated (no heating) to give 0.69 g (93%) of a clear pale yellow liquid which was used without further purification. ^{1}H NMR ($CDCl_3$, 300 MHz): δ 1.69 (br-s, 2H), 3.86 (s, 2H), 7.21−7.32 (m, 5H). ^{13}C{^{1}H} NMR ($CDCl_3$, 75.45 MHz): δ 46.4 (CH_2, J_{C-N} = 3.8 Hz), 126.7 (d), 127.0 (d), 128.5 (d), 143.2 (s).

***N*,*N*-Dimethylbenzylamine-[^{15}N].** Benzylamine-[^{15}N] (0.69 g, 6.4 mmol) and formaldehyde (1.9 mL, 25.5 mmol) were dissolved in 30 mL of MeOH. The solution was cooled to 0 °C, and $NaCNBH_3$ (0.56 g, 8.9 mmol) and $ZnCl_2$ (0.61 g, 4.5 mmol) in 20 mL of MeOH were added dropwise (slowly, 1 h). The solution was slowly warmed to room temperature over 2 h and then cooled to 0 °C, and NaOH (2 M, 50 mL) was added. The MeOH was removed and the residue extracted with ether (4 × 30 mL). Pentane was added and the solution washed with water (2 × 50 mL) and brine (1 × 50 mL) and dried (Na_2SO_4). The solvent was evaporated (no heating) to give 0.50 g (57%) of a clear yellow liquid. Kugelrohr distillation (85−95 °C, 20 Torr) gave 0.29 g (33%) of a clear, colorless liquid. ^{1}H NMR ($CDCl_3$, 300 MHz): δ 2.23 (d, J_{H-N} = 0.8 Hz, 6H), 3.41 (s, 2H), 7.24−7.33 (m, 5H). ^{13}C-{^{1}H} NMR ($CDCl_3$, 75.45 MHz): δ 45.2 (CH_3, J_{C-N} = 4.5 Hz), 64.3 (CH_2, J_{C-N} = 3.8 Hz), 127.0 (d), 128.2 (d), 129.1 (d), 138.7 (s). MS: M^+ = 136.1020 (calcd for $C_9H_{13}{}^{15}N$ = 136.1018).

Quantitation of Aryllithium Reagents. The concentrations of the aryllithium solutions were determined by the following methods: (1) quenching of the RLi solution with Me_2S_2 or Me_3SiCl and determination of the quantity of sulfide or silane produced by GC and/or proton NMR spectroscopy; (2) in some cases where the crude lithium reagent prepared by Li/Sn exchange was used, quantitative transmetalation was assumed; (3) HMPA has been shown to bind lithium reagents stoichiometrically in THF and ether solutions,[15j] thus the initial addition of HMPA or PMDTA to the aryllithium reagent was assumed to complex in stoichiometric fashion; integration of the complexed versus the noncomplexed species in the ^{6}Li NMR spectrum allowed determination of the aryllithium reagent concentration. Quantitative complexation was confirmed by examination of the ^{31}P NMR spectra for free HMPA.

2-Lithio-*N*,*N*-dimethylbenzylamine (1). A typical procedure for preparation of **1** (using the method of Hauser[1a]) is as follows: *N*,*N*-dimethylbenzylamine (2.99 g, 22.1 mmol) and 20 mL of ether were added to a dried and N_2-flushed 100-mL storage flask equipped with a stopcock and a septum. The solution was cooled to 0 °C, and 9.6 mL of 2.20 M *n*-BuLi in hexane (21.1 mmol, 0.95 equiv) was added dropwise. The resulting yellow solution was kept at room temperature for 7 d, during which time transparent crystals formed. The supernatant was removed by cannula transfer, and the crystals were washed with ether (3 × 15 mL). The crystals (87% yield) were used for the preparation of NMR samples or dissolved in THF to give a stock solution (typically 1.0−1.5 M) used for subsequent reactions. Similar procedures were used with *n*-Bu^{6}Li and/or ^{15}N-enriched *N*,*N*-dimethylbenzylamine.

An alternate method was also used. Et^{6}Li (0.304 g 8.67 mmol) was dissolved in 8.0 mL of ether. The solution was cooled to −78 °C, and *N*,*N*-dimethylbenzylamine (1.30 mL, 8.65 mmol) was added. The resulting clear yellow solution was warmed to room temperature and kept for 7 d. The supernatant was removed via cannula, and the crystals were washed with ether (3 × 15 mL) and dried in vaccuo. The crystals were stored in a glovebox until used.

After completion of the NMR experiment, some samples were quenched with Me_2S_2 to give *N*,*N*-dimethyl-2-(methylthio)benzylamine.[47] ^{1}H NMR ($CDCl_3$, 300 MHz): δ 2.26 (s, 6H), 2.46 (s, 3H), 3.46 (s, 2H), 7.07−7.15 (m, 1H), 7.16−7.31 (m, 3H). ^{13}C{^{1}H} NMR ($CDCl_3$, 75.4 MHz): δ 15.67 (CH_3), 45.37 (CH_3), 62.00 (CH_2), 124.22 (CH), 124.89 (CH), 127.63 (CH), 129.72 (CH), 136.61 (C), 138.71

(45) Watson, S. C.; Eastman, J. F. *J. Organomet. Chem.* **1967**, *9*, 165−168.

(46) Geller, B. A.; Samosvat, L. S. *J. Gen. Chem. (USSR)* **1960**, *30*, 1594−1597.

(C). MS (EI): $M^+ = 181.0924$ (calcd for $C_{10}H_{15}NS = 181.0925$). Yield was determined by GC analysis (HP 6890 with a 30 m × 0.33 mm × 0.25 μm EC-1 capillary column) against dodecane as internal standard.

Variable-Temperature Experiment of 1-[^{15}N,^{6}Li]. *N*,*N*-Dimethylbenzylamine-[^{15}N] (0.16 g, 1.16 mmol) and ether (1.7 mL) were added to a N_2-flushed 25-mL conical flask. The flask was cooled to 0 °C, and *n*-Bu^{6}Li (0.7 mL, 1.5 mmol) was added After 64 h, the supernatant was removed by cannula, and the crystals were washed with ether (3 × 1.5−2.0 mL). From the supernatant and washings, 0.044 g (28%) of ^{15}N-labeled *N*,*N*-dimethylbenzylamine was recovered. The washed crystals were dissolved in THF (1.5 mL) and ether (0.5 mL) and transferred by cannula to a dried and N_2-flushed 10-mm NMR tube. The reaction flask was rinsed with 0.3 mL of THF, which was also transferred into the NMR tube. The addition of Me_2O (1.0 mL) gave an aryllithium concentration of 0.28 M. The variable-temperature experiment was monitored by ^{6}Li, ^{15}N, and ^{13}C NMR spectroscopy. Spectra are shown in Figure 2. This sample was also used for a TMEDA titration (see below).

TMEDA and HMPA Titration of 1-[^{6}Li/^{15}N]. The sample from the variable-temperature study was titrated with TMEDA and monitored by ^{6}Li, ^{15}N, and ^{13}C NMR spectroscopy. An accurate molarity of the solution was unknown, but three portions of TMEDA were added: 80 μL, 0.54 mmol; 160 μL, 1.08 mmol; and 240 μL, 1.62 mmol (total 480 μL, 3.24 mmol). After the TMEDA titration, an excess of HMPA (480 μL, 2.76 mmol) was added, and ^{6}Li, ^{31}P, and ^{13}C spectra were acquired. A spectrum is shown in Figure 11. The probe temperature ranged from −125 to −135 °C during the experiment. The sample was quenched with MeOH/NH_4OAc to give *N*,*N*-dimethylbenzylamine-[^{15}N] (0.05 g, 0.35 mmol).

(Chloromethyl)dimethylsilyl(phenylthio)methane. Thioanisole (3.52 mL, 30.0 mmol) and TMEDA (4.64 mL, 30.0 mmol) were dissolved in THF (20 mL). The solution was cooled to 0 °C, 1.6 M *n*-BuLi (18.8 mL, 30.7 mmol) in pentane was added, and the solution was stirred for 1 h. In a second flask, chloro(chloromethyl)dimethylsilane (5.2 mL, 32.0 mmol) was dissolved in THF (35 mL). The solution was cooled to −78 °C, and the phenylthiomethyllithium solution was added slowly via cannula and stirred for 5 min. Hexanes (200 mL) and water (500 mL) were added, and the water layer was extracted with hexanes (1 × 100 mL). The organic layer was washed with water (2 × 30 mL) and dried (Na_2SO_4), and the solvent was evaporated. Kugelrohr distillation (100−120 °C, 1−2 mm) gave 6.17 g (89%) of a colorless liquid. ^{1}H NMR (200.132 MHz, $CDCl_3$): $\delta = 0.28$ (s, 6H), 2.32 (s, 2H), 2.90 (s, 2H), 7.07−7.18 (m, 1H), 7.22−7.32 (m, 4H). ^{13}C{^{1}H} NMR (90.556 MHz, $CDCl_3$): $\delta = -4.7$ (2C, $SiMe_2$), 15.6 (SCH_2Si), 29.3 ($SiCH_2Cl$), 125.0 (*p*), 126.5 (2C, *m*), 128.7 (2C, *o*), 139.3 (*i*). MS (EI): $M^+ = 230.0355$ (calcd for $C_{10}H_{15}ClSSi = 230.0352$).

Dimethyl(*N*-pyrrolidinomethyl)silyl(phenylthio)methane (Precursor for 14). (Chloromethyl)dimethylsilyl(phenylthio)methane (690 mg, 3.0 mmol) was refluxed in pyrrolidine (7 mL) for 3 h. Excess pyrrolidine was evaporated, and the residue was emulsified in CH_2Cl_2 (2 mL) and hexanes (2 mL). The emulsion was purified by column chromatography (200 mL of 95:5 hexanes/ethyl acetate followed by 250 mL of 90:5:5 hexanes/ethyl acetate/triethylamine), yielding 703 mg (2.65 mmol, 88%) of a light yellow liquid. ^{1}H NMR (200.132 MHz, $CDCl_3$): $\delta = 0.23$ (s, $^{2}J_{Si-H} = 6.7$ Hz, 6H), 1.73−1.80 (m, 4H), 2.16 (s, $^{2}J_{Si-H} = 5.5$ Hz, 2H), 2.25 (s, $^{2}J_{Si-H} = 6.4$ Hz, 2H), 2.42−2.54 (m, 4H), 7.06−7.17 (m, 1H), 7.22−7.32 (m, 4H). ^{13}C{^{1}H} NMR (90.556 MHz, $CDCl_3$): $\delta = -3.1$ (2C, $^{1}J_{Si-C} = 39$ Hz, $SiMe_2$), 16.9 (1C, $^{1}J_{Si-C} = 46$ Hz, SCH_2Si), 23.9 (2C, β-pyrrolidine), 45.8 (1C, $^{1}J_{Si-C} = 59$ Hz, $SiCH_2N$), 58.0 (2C, α-pyrrolidine), 124.5 (*p*), 126.1 (2C, *m*), 128.5 (2C, *o*), 140.1 (*i*). MS (EI): $M^+ = 265.1318$ (calcd for $C_{14}H_{23}NSSi = 265.1320$).

HMPA Titration of 14:15 (1:1 Mixture). A solution of **14** and **15** (each 0.09 M) in a 10-mm NMR tube was prepared by metalating a solution of trimethylsilyl(phenylthio)methane (78 μL, 0.30 mmol) and dimethyl(*N*-pyrrolidinomethyl)silyl(phenylthio)methane (61 μL, 0.30 mmol) in ether (1.2 mL) and THF (1.8 mL) at −78 °C with 1.7 M *t*-BuLi (0.35 mL, 0.60 mmol) in pentane. The NMR tube was warmed to −20 °C for 4 d. ^{7}Li, ^{6}Li, and ^{31}P NMR spectra were acquired at 0, 0.2, 0.4, 0.6, 0.8, 1, 1.2, 1.5, and 2 equiv of HMPA. The probe temperature was −113 °C during the experiment. The data summarized in Table 2 were obtained by using the integrations from the ^{31}P and ^{7}Li NMR spectra.

Table 2. Competitive Titration of **14** and **15** with HMPA

equiv HMPA	% **14**	% **14**-h_1[a]	% **15**	% **15**-h_1	(% **14**-h_1)/(% **15**-h_1)	K_{eq}[b]
0	58		42			
0.2	40	18	39	3	6.1	5.9
0.4	24	34	34	8	4.1	6.0
0.6	12	46	25	17	2.7	5.6
0.8	4	54	13	29	1.9	6.0

[a] h = HMPA. [b] $K_{eq} = [\mathbf{14}][\mathbf{15}\text{-}h_1]/[\mathbf{14}\text{-}h_1][\mathbf{15}]$.

Acknowledgment. We thank the National Science Foundation for financial support of this work, and Prof. Gideon Fraenkel for assistance in development of the exchange matrixes used for the NMR line shape analyses of the intermolecular exchange processes of **1**.

Supporting Information Available: Experimental procedures for the preparation of **2** (^{15}N labeled), **3**, **4** (^{15}N labeled), **5**, **16**, **17**, and **18**; data and spectra from variable-temperature NMR experiments and simulations on **1**, **2**, and **13**; spectra and data from the variable-concentration NMR studies of **1** and **4**; spectra from HMPA titrations of **2**, **3**, **4**, and **13**; spectra and data for competitive NMR titration of **16**/**17** and **18**/**15**; NMR spectra and data for TMEDA and PMDTA titrations of **1** and **5**; X-ray crystal structure data for **3** (PDF). This material is available free of charge via the Internet at http://pubs.acs.org.

JA010489B

(47) Ohkata, K.; Takee, K.; Akiba, K. *Tetrahedron Lett.* **1983**, *24*, 4859−4862.